ATF6 Decreases Myocardial Ischemia/Reperfusion Damage and Links ER Stress and Oxidative Stress Signaling Pathways in the Heart

Jung-Kang Jin, Erik A. Blackwood, Khalid Azizi, Donna J. Thuerauf, Asal G. Fahem, Christoph Hofmann, Randal J. Kaufman, Shirin Doroudgar, Christopher C. Glembotski

Rationale: **Endoplasmic reticulum (ER) stress causes the accumulation of misfolded proteins in the ER, activating the transcription factor, ATF6 (activating transcription factor 6 alpha), which induces ER stress response genes. Myocardial ischemia induces the ER stress response; however, neither the function of this response nor whether it is mediated by ATF6 is known.**

Objective: **Here, we examined the effects of blocking the ATF6-mediated ER stress response on ischemia/reperfusion (I/R) in cardiac myocytes and mouse hearts.**

Methods and Results: **Knockdown of ATF6 in cardiac myocytes subjected to I/R increased reactive oxygen species and necrotic cell death, both of which were mitigated by ATF6 overexpression. Under nonstressed conditions, wild-type and ATF6 knockout mouse hearts were similar. However, compared with wild-type, ATF6 knockout hearts showed increased damage and decreased function after I/R. Mechanistically, gene array analysis showed that ATF6, which is known to induce genes encoding ER proteins that augment ER protein folding, induced numerous oxidative stress response genes not previously known to be ATF6-inducible. Many of the proteins encoded by the ATF6-induced oxidative stress genes identified here reside outside the ER, including catalase, which is known to decrease damaging reactive oxygen species in the heart. Catalase was induced by the canonical ER stressor, tunicamycin, and by I/R in cardiac myocytes from wild-type but not in cardiac myocytes from ATF6 knockout mice. ER stress response elements were identified in the catalase gene and were shown to bind ATF6 in cardiac myocytes, which increased catalase promoter activity. Overexpression of catalase, in vivo, restored ATF6 knockout mouse heart function to wild-type levels in a mouse model of I/R, as did adeno-associated virus 9–mediated ATF6 overexpression.**

Conclusions: **ATF6 serves an important role as a previously unappreciated link between the ER stress and oxidative stress gene programs, supporting a novel mechanism by which ATF6 decreases myocardial I/R damage.**

(*Circ Res*. 2017;120:862-875. DOI: 10.1161/CIRCRESAHA.116.310266.)

Key Words: ATF6 ■ cardiac myocyte ■ catalase ■ endoplasmic reticulum stress ■ ischemia ■ ischemia/reperfusion injury ■ oxidative stress ■ protein folding ■ unfolded protein response

Cellular function depends on protein homeostasis, also known as proteostasis.[1] Proteostasis requires the efficient folding of newly synthesized proteins, as well as protein quality control and degradation, which decrease the accumulation of misfolded, potentially toxic proteins.[1] At least one third of all proteins, including calcium-handling proteins, transmembrane receptors, growth factors, and hormones, are synthesized, modified, and folded in the endoplasmic reticulum (ER), then trafficked to various membrane compartments, or secreted.[2] Thus, the environment in the ER must be optimal for efficient synthesis and folding of these important proteins.[3–5]

Editorial, see p 759
In This Issue, see p 745

A variety of diseases, including many that affect the heart, challenge ER protein–folding capacity.[6–9] Such challenges can be caused by mutations in genes that encode ER proteins, which can affect their folding or targeting, or by disease-related perturbations of the ER environment,[10] which lead to imbalanced proteostasis, in extreme cases causing ER stress. ER

Original received November 2, 2016; revision received December 2, 2016; accepted December 8, 2016. In November 2016, the average time from submission to first decision for all original research papers submitted to *Circulation Research* was 15.7 days.

From the San Diego State University Heart Institute and the Department of Biology, San Diego State University, CA (J.-K.J., E.A.B., K.A., D.J.T., A.G.F., C.H., S.D., C.C.G.); Department of Cardiology, Angiology, and Pneumology, University Hospital Heidelberg, Germany (C.H., S.D.); DZHK (German Centre for Cardiovascular Research), Partner Site Heidelberg/Mannheim, Heidelberg, Germany (C.H., S.D.); and Degenerative Diseases Program, Sanford Burnham Prebys Medical Discovery Institute, La Jolla, CA (R.J.K.).

The online-only Data Supplement is available with this article at http://circres.ahajournals.org/lookup/suppl/doi:10.1161/CIRCRESAHA.116.310266/-/DC1.

Correspondence to Christopher C. Glembotski, SDSU Heart Institute and Department of Biology, San Diego State University, 5500 Campanile Dr, San Diego, CA 92182. E-mail cglembotski@mail.sdsu.edu

Novelty and Significance

What Is Known?

- Myocardial ischemia causes endoplasmic reticulum (ER) stress and the misfolding of proteins in the ER of cardiac myocytes, which activates the ER stress response transcription factor, ATF6 (activating transcription factor 6 alpha).
- ATF6 increases expression of ER proteins, such as chaperones that restore ER protein folding, thus, avoiding the toxic effects of misfolded proteins.
- Ischemia/reperfusion (I/R) damage in the heart, which is caused mainly by increased reactive oxygen species, is decreased by ATF6; however, the mechanism is unknown.

What New Information Does This Article Contribute?

- ATF6 induces numerous antioxidative stress genes, such as catalase, which is known to decrease reactive oxygen species and reduce I/R damage in the heart.
- ATF6-mediated catalase induction contributes to the ability of ATF6 to protect against I/R damage.
- ATF6 links ER stress to oxidative stress in the heart

The ER is the site of secreted and membrane protein synthesis and folding, thus, serving a critical role in cardiac myocyte function. ER protein folding is impaired in the ischemic heart, which contributes to pathology. Impaired ER protein folding activates the ER stress transcription factor, ATF6, which decreases I/R damage in the heart. However, because most known ATF6-induced proteins function to enhance protein folding in the ER, it is unknown how ATF6 can decrease myocardial I/R damage, most of which is caused by reactive oxygen species. Here we used ATF6 gain- and loss-of-function approaches to show that during I/R, ATF6 is not only required for induction of ER-resident proteins that enhance protein folding in the ER, but surprisingly is also responsible for inducing numerous oxidative stress response genes that encode antioxidant proteins, such as catalase, which do not reside in the ER. ATF6-mediated catalase induction was found to contribute to the protective effects of ATF6. These results show that antioxidant proteins are induced by ATF6 during ER stress and reveal a new function for ATF6 as a link between the ER stress and oxidative stress in the heart.

Nonstandard Abbreviations and Acronyms

ATF6	activating transcription factor 6 alpha
ATF6 KO	ATF6 alpha knockout
ER	endoplasmic reticulum
Grp94	94 kilodalton glucose-regulated protein
Grp78	78 kilodalton glucose-regulated protein
I/R	ischemia/reperfusion
NRVM	neonatal rat ventricular myocytes
PDIA6	protein disulfide isomerase family A, member 6
ROS	reactive oxygen species
sI/R	simulated ischemia/reperfusion
TM	tunicamycin

stress contributes to pathology by impeding the production of critical ER proteins and by increasing the accumulation of potentially toxic misfolded proteins.

ER protein misfolding activates the ER stress response, a conserved signaling system that initiates multiple processes, including gene programs that initially restore proteostasis, thus serving adaptive roles. However, if the ER stress is not resolved by these initial processes, continued ER stress leads to cell death.[8,11,12] Roles for the ER stress response in either mitigating or causing damage during diseases, including ischemic heart disease, are not well understood.[13] Therefore, defining the molecular processes in the diseased heart that are regulated by ER stress, as well as understanding how and when ER stress is activated in the heart, are required to determine whether to use ER stress–activating or ER stress–inhibiting strategies to improve cardiac function during pathology.

ER stress response genes are regulated by several transcription factors, including ATF6α (activating transcription factor 6 alpha), abbreviated here as ATF6, a 670 amino acid, ER-transmembrane protein.[14,15] Although not well studied in cardiac myocytes, in model cell lines, ER protein misfolding triggers the translocation of ATF6 to the nucleus, where it induces ER stress response genes (Figure 1A).[15] Most of these genes encode proteins, such as the well-studied ER chaperone, GRP78 (glucose-regulated protein 78 kDa), that are localized to the ER, where they enhance ER protein folding and contribute to resolving the ER stress. To examine roles for ATF6 in the heart, we previously generated a transgenic mouse that expresses a conditionally activated form of ATF6 in cardiac myocytes; in these mice, we showed that activation of ATF6 increased the expression of numerous genes, including *Grp78*, and decreased myocardial ischemia/reperfusion (I/R) damage.[16,17] Although this showed that ectopically expressed ATF6 can be adaptive in the heart, the function of endogenous ATF6 in the heart has not been studied. Moreover, because most known ATF6-induced proteins localize to the ER, where they enhance protein-folding,[18] it is unclear how ATF6-regulated genes could decrease I/R damage in the heart, most of which is caused by reactive oxygen species (ROS) generated outside the ER.[19,20] Here, we examined the effects of gene-targeted disruption of endogenous ATF6 and showed that it increased myocardial I/R damage. Mechanistically, we found that during I/R, ATF6 is required for the induction of numerous oxidative stress response genes that encode antioxidant proteins, many of which reside outside the ER. This is the first study of ATF6 gene deletion in the heart and the first to show in any cell or tissue type that ATF6 is a key transcriptional inducer of oxidative stress response genes encoding proteins outside the ER that decrease damaging ROS during I/R.

Methods

Further details on the Methods can be found in the Online Data Supplement.

Laboratory Animals

The research reported in this article has been reviewed and approved by the SDSU Institutional Animal Care and Use Committee, and it

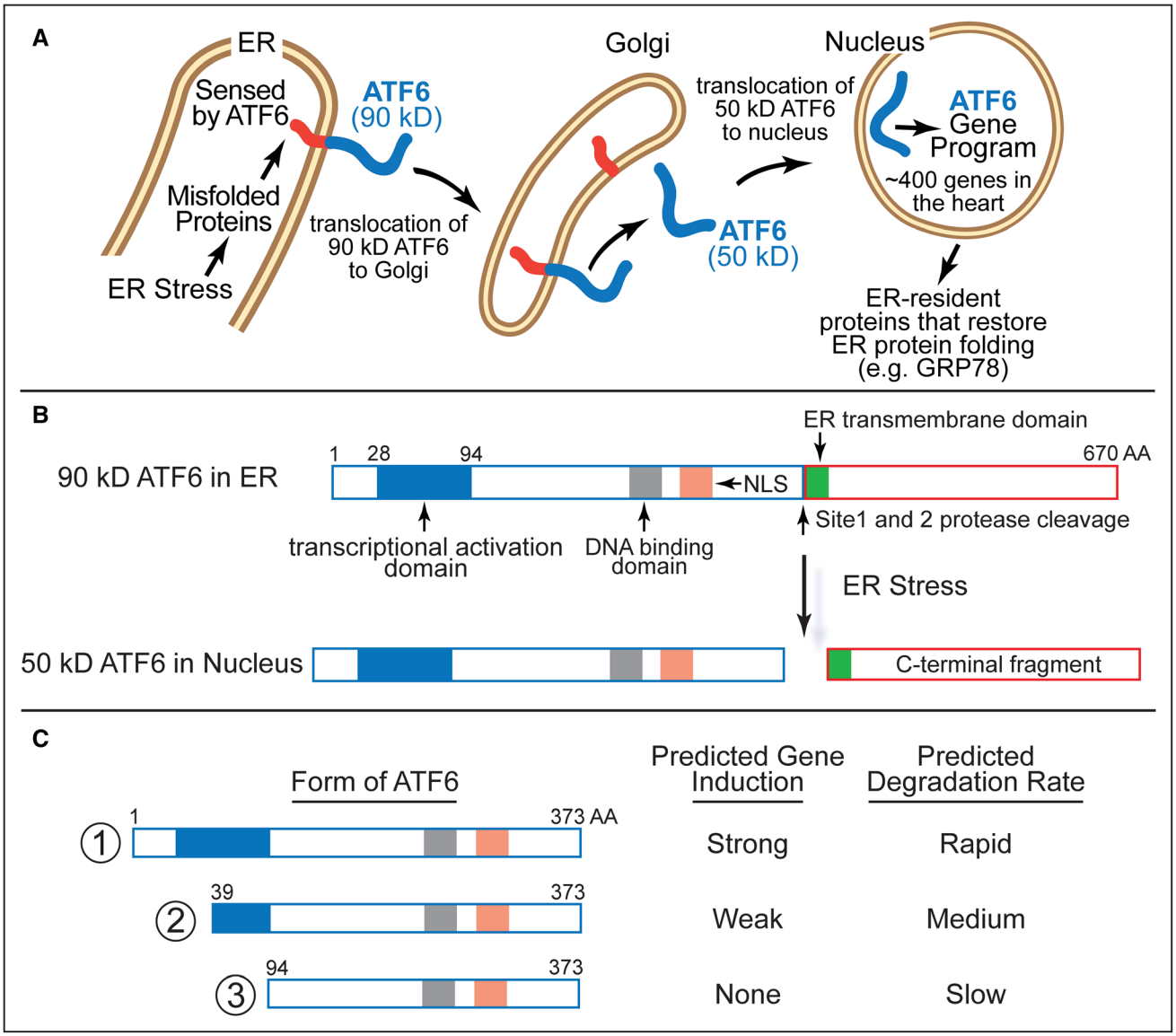

Figure 1. ATF6 activation by ER stress. A, Inactive ATF6 is a 90-kDa ER transmembrane protein that is released from the ER by protein misfolding and translocates to the Golgi, where it is cleaved by site 1 and site 2 proteases to liberate a 50-kDa N-terminal fragment, which translocates to the nucleus and acts as a transcription factor to regulate the ATF6 gene program. **B**, Shown are the relative locations of the ATF6 transcriptional activation domain (blue), DNA-binding domain, nuclear localization sequence (NLS), site 1 and site 2 protease cleavage sites, and ER transmembrane domains in full-length, p90 ATF6 (670 amino acids), as well as the location where ATF6 is cleaved by ER stress. **C**, Shown are the N-terminal truncated forms of active ATF6 used in this study. Form 1 represents the native ATF6 with the transcriptional activation, DNA binding, and nuclear localization domains intact, while forms 2 and 3 have progressive truncations through the transcriptional activation domain. Also shown is the predicted relative strength of gene induction and the predicted degradation rate of each form. ATF6 indicates activating transcription factor 6 alpha; ER, endoplasmic reticulum; and GRP78, glucose-regulated protein 78 kDa.

conforms to the Guide for the Care and Use of Laboratory Animals published by the National Research Council.

ATF6 Knockout Mice

There are 2 isoforms of ATF6, ATF6α and ATF6β. The mice used in this study were generated so that ATF6α, which is expressed in all cell types, has been globally deleted in all tissues.[21] In that study, it was found that ATF6α deletion had no effect on development through at least 4 months of age. Because ATF6β was not examined in this study, in most cases in this article, we use the term ATF6 to mean ATF6α. ATF6α-floxed mice were unavailable at the time of this study. The ATF6 knockout mice used in this study were 10-week-old males.

Statistics

Unless otherwise stated, values shown are mean±SEM, and statistical treatments are either *t* test or one-way analysis of variance followed by Newman–Keuls post hoc analysis.

Results

Though not well studied in cardiac myocytes, in model cell lines, it has been shown that the 90-kDa ER form of ATF6 senses misfolded proteins in the ER, then translocates to the Golgi where it is cleaved to liberate an N-terminal fragment in the cytosol that has a nuclear localization sequence and a DNA-binding domain (Figure 1B). The N-terminal 50-kDa

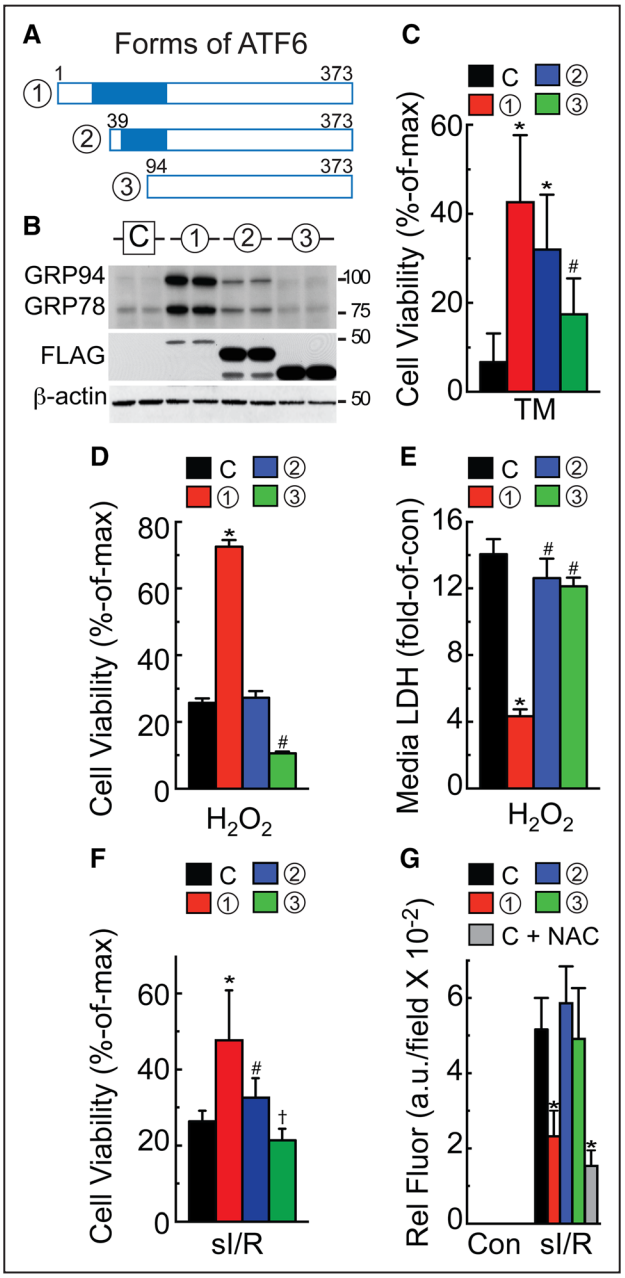

Figure 2. Effects of ATF6 overexpression on ER and oxidative stress in cultured cardiac myocytes. A, Diagram of the forms of ATF6 used in this study. **B,** Neonatal rat ventricular myocytes (NRVM) were infected with adenovirus (AdV) encoding either no protein (C) or 1 of the 3 forms of ATF6 shown, then immunoblotted using a FLAG antibody to detect the overexpressed ATF6, a KDEL antibody, which detects GRP94 and 78, or β-actin antibody. **C–G,** NRVM were infected with either control (C) or each of the ATF6-expressing AdV shown in **A**, then treated for 48 h with TM (40 μg/mL; **C**), 37.5 μmol/L H_2O_2 for 8 h (**D** and **E**), sI/R (**F** and **G**), and 5 mmol/L N-acetyl cysteine (NAC; **G**), followed by viability determination using an MTT ((3-(4,5-dimethylthiazol-2-yl)-2,5-diphenyltetrazolium bromide) tetrazolium) assay, or by media enzyme assay to determine LDH (lactate dehydrogenase) activity, or ROS measurement with CellROX, as shown. *#†$P \leq 0.05$, different than other values by analysis of variance (ANOVA). ATF6 indicates activating transcription factor 6 alpha; ER, endoplasmic reticulum; GRP78, glucose-regulated protein 78 kDa; GRP94, 94 kDa glucose-regulated protein; ROS, reactive oxygen species; sI/R, simulated ischemia/reperfusion; and TM, tunicamycin.

fragment of ATF6, which is ≈400 amino acids, translocates to the nucleus where it functions as a transcription factor.[22] Using HeLa cells as a model, we previously mapped the transcriptional activation domain of ATF6 to a region between amino acids 29–94.[23] However, there have been no studies examining the ATF6 transcriptional activation domain in cardiac myocytes or in the heart. Accordingly, here we generated expression constructs that encode 3 forms of ATF6 that we predicted from our studies with HeLa cells to exhibit a range of transcriptional activities (Figure 1C).

Initial studies in neonatal rat ventricular myocytes (NRVM) showed that the 3 forms of ATF6 (Figure 2A) exhibited different abilities to increase expression of the well-known ATF6-induced proteins, GRP94 (94 kDa glucose-regulated protein) and GRP78. The native N-terminal fragment of ATF6, ATF6(1–373), called form 1 here, which was expressed at approximately similar levels as endogenous ATF6 (Online Figure IA), mimics the cleaved form of ATF6 and was the most potent inducer, while ATF6(39–373), form 2, which has about half of the transcriptional activation domain missing, was partially active and ATF6(94–373), form 3, which lacks all of the transcriptional activation domain, was inactive (Figure 2B; GRP94 and GRP78). None of the 3 forms of ATF6 affected the other 2 branches of the ER stress response because they did not increase PERK (PKR-like ER-localized eIF2α kinase) phosphorylation, nor did they induce XBP1 (X-box binding protein 1) splicing, an indicator of IRE1 (inositol requiring gene 1) activation (Online Figure IB). We also previously showed in HeLa cells that ATF6 exhibits a novel degraded-when-active property, such that the more transcriptionally active forms of ATF6 exhibit the shortest half-lives (Figure 1C).[23,24] Consistent with those studies were our findings in NRVM, showing that the transcriptional activity of ATF6 was inversely related to the expression level of ATF6 (Figure 2B; FLAG).

Given the differential effects of these forms of ATF6 on ER stress gene induction, they are potentially valuable reagents with which to discover cardiac myocyte functions that are regulated by ATF6-induced genes. For example, if these forms of ATF6 affect a particular myocyte function, such as survival, with the same rank order that they affect ATF6 target gene expression, then it is likely that at least some ATF6 target genes contribute to those functions. As an example, we showed that in NRVM treated with the prototypical ER stressor, tunicamycin (TM), which induces ER protein misfolding by inhibiting protein glycosylation, the 3 forms of ATF6 decreased ER stress–induced cell death with the same rank order that they induce ER proteins that reduce ER protein misfolding, for example, GRP94 and GRP78 (Figure 2C).

Next, we examined the effects of other stressors that are not typically considered to be inducers of ER protein misfolding and the canonical ER stress response, such as H_2O_2, which induces oxidative stress by increasing ROS levels. Although ATF6 was expected to protect against ER stress–induced cell death, which is primarily apoptotic, we anticipated that it would be ineffective against oxidative stress–induced cell death, which is primarily necrotic. Surprisingly, form 1

of ATF6 protected myocytes from H_2O_2-induced cell death (Figure 2D, red), form 2 was without effect (Figure 2D, blue), while form 3, which exerts dominant-negative effects on endogenous ATF6 signaling, actually increased H_2O_2-induced myocyte death (Figure 2D, green). It is unclear why the relative effects of the 3 forms of ATF6 are somewhat different in response to TM versus H_2O_2, but one possibility is that the effects of ATF6 on H_2O_2-induced myocyte death might be the result of induction of proteins that do not reside in the ER and do not directly affect ER protein folding, such as antioxidant genes. Because ATF6 is not known for its ability to affect the expression of antioxidant genes, we focused in more depth on the antioxidant effects of ATF6.

It has been shown that H_2O_2 kills myocytes by necrosis[25]; accordingly, we examined the effects of the 3 forms of ATF6 on the media levels of LDH (lactate dehydrogenase) and HMGB1 (high mobility group protein B1), which are measures of necrosis.[25,26] Again, form 1 of ATF6 strongly decreased media levels of LDH and HMGB1, while the other forms had less of an effect (Figure 2E; Online Figure IC), indicating that activated ATF6 can inhibit H_2O_2-induced necrosis of cardiac myocytes. Consistent with this was our finding that H_2O_2 had no effect on NAD(+) ADP-ribosyltransferase cleavage, a measure of apoptosis[27] (Online Figure ID and IE). Because the deleterious effects of H_2O_2 are caused by ROS, we tested the 3 forms of ATF6 in NRVM subjected to simulated ischemia/reperfusion (sI/R), a pathophysiological maneuver that increases mitochondrial-derived ROS (Online Figure IF). Similar to the findings with H_2O_2, form 1 of ATF6 exhibited the most significant ability to protect cardiac myocytes from sI/R-mediated death (Figure 2F) and to decrease ROS generation during sI/R (Figure 2G; Online Figure IG). Moreover, N-acetyl cysteine, a well-characterized ROS scavenger, mimicked the ability of form 1 of ATF6 to decrease ROS when examined using 2 different assays, as recently recommended[28] (Figure 2G; Online Figure IG; sI/R N-acetyl cysteine), indicating that ATF6 acted functionally like an ROS scavenger.

These findings suggested that there might be a previously unappreciated link between ER stress signaling by ATF6 and ROS reduction; moreover, because the damaging ROS produced during reperfusion are mostly generated in mitochondria,[29] the link could involve ATF6-mediated decreases in total cellular ROS. To examine whether this link also existed between endogenous ATF6 and ROS levels, NRVM were treated with siRNA to knockdown endogenous ATF6. Immunoblots showed that 2 different ATF6 siRNAs decreased the levels of full-length, p90 ATF6 and resulted in the absence of cleaved, p50 ATF6 on TM treatment (Figure 3A, p90 and p50 ATF6 lanes 5–8; Online Figure IIA). Importantly, siRNA-mediated ATF6 knockdown also blunted the induction of ATF6-inducible target genes, Grp94, Grp78, and PDIA6 (protein disulfide isomerase family A, member 6; Figure 3A; GRP94, GRP78, PDIA6, lanes 5–8; Online Figure IIA), but had no effect on the basal activity of the other 2 branches of the ER stress response that are mediated by PERK and IRE1 (Online Figure IIB). Endogenous ATF6 is difficult to detect. Accordingly, to ensure that the bands observed in Figure 3A and Online Figure IIA were bona fide endogenous p90 and p50 ATF6, we validated a variety of commercially available antibodies using known controls in which we knew p90 and p50 ATF6 were expressed (Online Figure III).

ATF6 knockdown decreased cell viability in NRVM treated with either TM (Figure 3B) or H_2O_2 (Figure 3C). Moreover, ATF6 knockdown increased necrotic cell death in response to H_2O_2 treatment, as determined by increased media levels of LDH (Figure 3D) and HMGB1 (Online Figure IIC). Simulated ischemia was shown to activate ATF6 and downstream genes in NRVM, as evidenced by the conversion of p90 ATF6 to p50 ATF6 and the increased levels of canonical ATF6 target proteins, GRP94, GRP78, and PDIA6 (Figure 3E, sI). ATF6 activation appeared to persist during sI/R (Figure 3E, sI/R). Moreover, immunocytofluorescence showed that ATF6 adopted a diffuse staining pattern in normoxic NRVM, consistent with a sarcoplasmic reticulum/ER, non-nuclear localization, while after sI (not shown) or sI/R (Online Figure IV), ATF6 was found almost exclusively in nuclei. ATF6 knockdown decreased viability in NRVM subjected to I/R, increased media levels of LDH and HMGB1, increased ROS levels, and increased malondialdehyde, the latter of which is a measure of ROS-associated lipid peroxidation[30] (Figure 3F through 3I; Online Figure IID through IIG). Treatment with N-acetyl cysteine verified that ROS were generated by sI/R (Figure 3H; Online Figure IIF). Thus, endogenous ATF6 protected NRVM from the maladaptive effects of prolonged ER protein misfolding and ER stress by TM, as well as from the damaging effects of oxidative stress induced by H_2O_2 and sI/R.

The effects of ATF6 deletion in the mouse heart have not been previously examined; therefore, to assess the effects of deleting ATF6, in vivo, ATF6 knockout mice (KO)[21] were used. Immunoblots confirmed the absence of p90 ATF6 in ATF6 KO mouse hearts compared with wild-type (WT) mouse hearts (Figure 4A). The ATF6 KO mice do not exhibit any overt phenotype under nonstressed conditions, developing normally through adulthood.[21] Echocardiography confirmed that this was the case in the heart, demonstrating that all cardiac dimensions and contractile properties of the ATF6 KO mice were the same as the WT mice (Online Table I). When mice were subjected to a model of surgical coronary artery occlusion for 30 minutes followed by reperfusion for 24 hours, the area at risk was the same for both lines; however, infarct sizes were significantly larger in ATF6 KO mice after I/R (Figure 4B). Moreover, after I/R, plasma LDH levels and tissue malondialdehyde levels were greater in ATF6 KO mice than in WT mice (Figure 4C and 4D). Immunocytofluorescence and immunoblots of mouse heart tissue sections showed that I/R increased ATF6 and GRP78 in WT mice, but not in ATF6 KO mice (Online Figures V and VI). Moreover, I/R did not activate PERK or IRE1, as shown by the absence of phosphorylated PERK and spliced XBP1 (Online Figure VII). Additionally, examination of heart extracts for transcript levels of canonical ATF6-regulated genes showed that compared with WT mouse hearts, there was 50% or less Grp94, Grp78, and PDIA6 mRNA in ATF6 KO mouse hearts (Figure 4E).

We also examined whether the effects of ATF6 deletion seen in vivo could be recapitulated in isolated hearts subjected

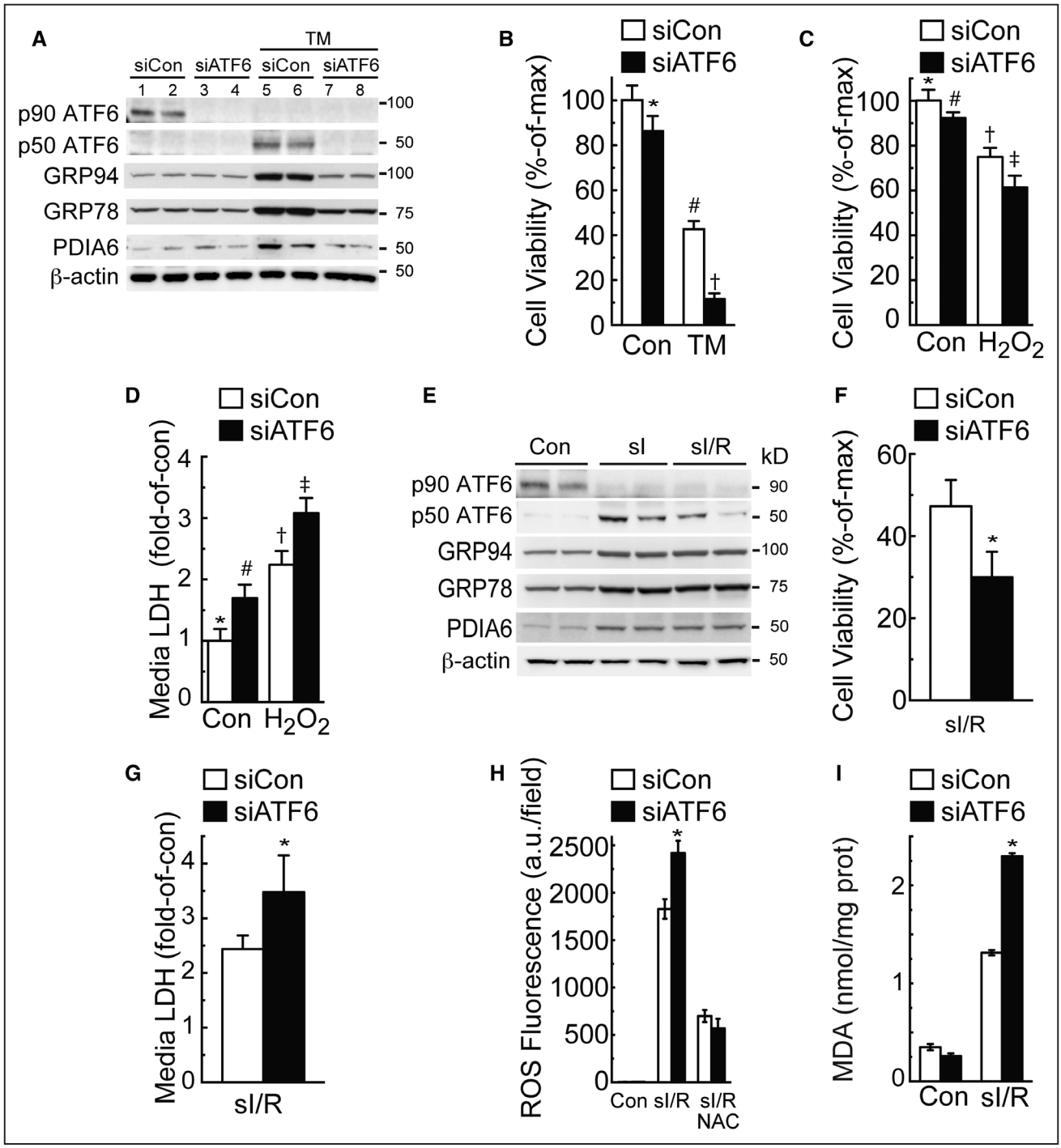

Figure 3. Effects of ATF6 knockdown on ER stress and oxidative stress in cultured cardiac myocytes. A, NRVM were transfected with a nontargeted siRNA (siCon) or an siRNA targeted to rat ATF6 (siATF6), and then treated without or with TM (10 μg/mL) for 24 h, then immunoblotted for endogenous ATF6 (p90 and p50 ATF6), GRP94, GRP78, PDIA6, and β-actin. Note that this figure is replicated in Online Figure IIA with the addition of a second siRNA to ATF6. NRVM were treated similarly with siCon or siATF6 for all subsequent experiments in this figure, except (**E**). **B,** NRVM were treated for 48 h without or with TM (40 μg/mL) followed by MTT ((3-(4,5-dimethylthiazol-2-yl)-2,5-diphenyltetrazolium bromide) tetrazolium) for cell viability. *#†$P \leq 0.05$, different from other values by analysis of variance (ANOVA). **C and D**, NRVM were treated for 8 h with 37.5 μmol/L H_2O_2, then examined by MTT for cell viability (**C**) or media assayed for LDH (lactate dehydrogenase) activity (**D**). *#†‡$P \leq 0.05$, different than other values by ANOVA. **E,** NRVM were subjected to Con, sI, or sI/R, then extracts were immunoblotted for the proteins shown. **F–I,** NRVM were treated with sI/R then examined by calcein blue AM for cell viability, media LDH activity, ROS using CellROX, and malondialdehyde (MDA). *$P \leq 0.05$, different from siCon by *t* test. ATF6 indicates activating transcription factor 6 alpha; ER, endoplasmic reticulum; GRP78, glucose-regulated protein 78 kDa; GRP94, 94 kDa glucose-regulated protein; NRVM, neonatal rat ventricular myocytes; ROS, reactive oxygen species; sI/R, simulated ischemia/reperfusion; and TM, tunicamycin.

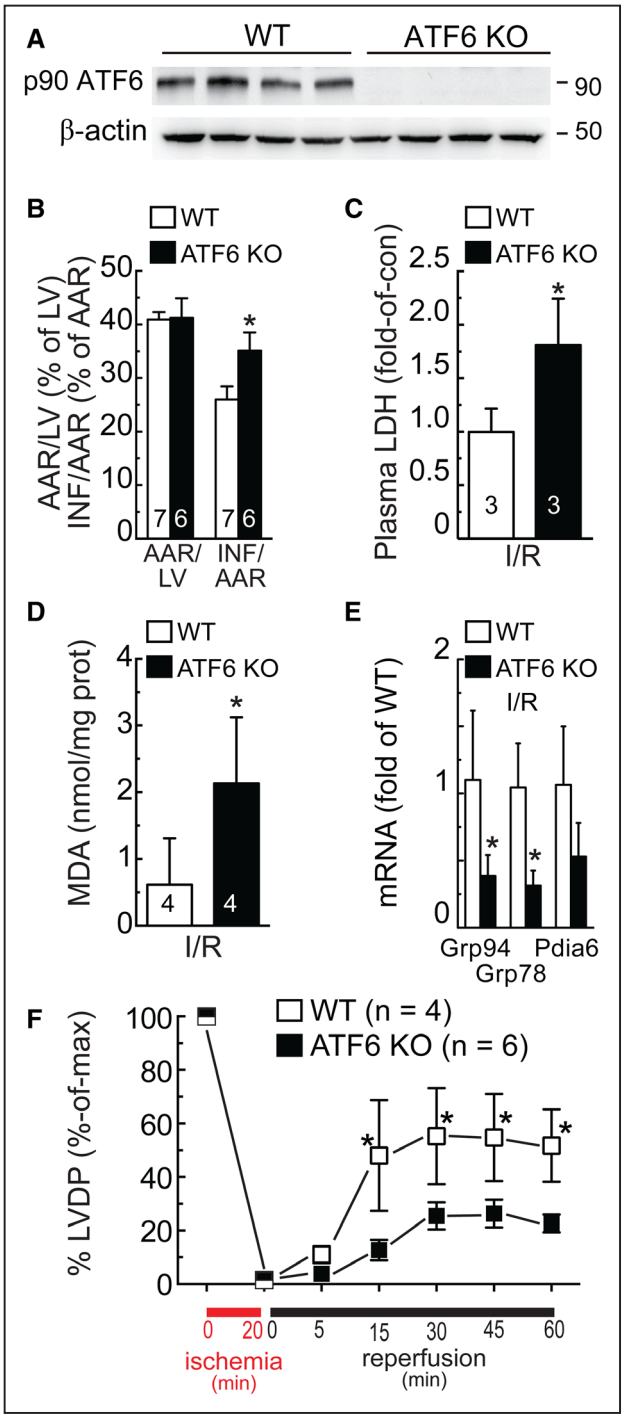

Figure 4. Effect of ATF6 gene deletion in hearts subjected to ischemia/reperfusion. A, WT (n=4) or ATF6 KO (n=4) mouse heart extracts were examined for ATF6 and β-actin by immunoblotting. To detect p90 ATF6 in mouse heart extracts, the antibody raised against the C-terminal of ATF6 was used. **B,** WT (n=7) or ATF6 KO (n=6) mice were subjected to in vivo I/R, then hearts were assessed for damage; *$P \leq 0.05$, different than WT INF/AAR by *t* test. **C,** Plasma from WT (n=3) and ATF6 KO (n=3) mice assessed for LDH (lactate dehydrogenase). *$P \leq 0.05$, different than WT by *t* test. **D,** Heart extracts from WT (n=4) and ATF6 KO (n=4) mice assessed for malondialdehyde (MDA),*$P \leq 0.05$, different than WT by *t* test. **E,** WT (n=3) and ATF6 KO (n=4) mouse hearts were subjected to in vivo I/R after which heart extracts were analyzed for Grp94, Grp78, and Pdia6 mRNA levels, normalized to β-actin mRNA by quantitative (*Continued*)

Figure 4. Continued reverse transcriptase polymerase chain reaction (qRT-PCR), *$P \leq 0.05$, different than WT for each gene target by *t* test. **F,** WT (n=4) and ATF6 KO (n=6) mouse hearts were subjected to ex vivo global ischemia/reperfusion, and left ventricular developed pressure (LVDP) was determined before and after ischemia and presented as percent of maximal function observed during equilibration for each mouse line, *$P \leq 0.05$, different than ATF6 KO by *t* test. AAR indicates area at risk; ATF6, activating transcription factor 6 alpha; GRP78, glucose-regulated protein 78 kDa; GRP94, 94 kDa glucose-regulated protein; INF, infarcted area; I/R, ischemia/reperfusion; KO, knockout; LV, left ventricle; and WT, wild-type.

to ex vivo I/R. Compared with WT mouse hearts, ATF6 KO mouse hearts were more susceptible to a loss of cardiac function after global ischemia, exhibiting a significantly reduced recovery of left ventricular developed pressure on reperfusion (Figure 4F). Thus, the effects of global ATF6 deletion on I/R damage were autonomous to the heart.

Next we examined the effects of ATF6 deletion in adult cardiac myocytes isolated from ATF6 KO mouse hearts. Immunocytofluorescence showed that myocytes from WT mouse hearts exhibited low levels of ATF6 under basal conditions; however, on TM treatment, ATF6 increased in WT mouse myocytes and localized throughout the cell, as well as in the nucleus (Online Figure VIIIA and VIIIB). In contrast, ATF6 KO mouse myocytes did not exhibit any detectible ATF6 under basal conditions or when treated with TM (Online Figure VIIIC and VIIID). Examination of the ATF6 target gene product, GRP78, was consistent with these results; in WT mouse myocytes, GRP78 levels increased in response to TM (Online Figure IXA and IXB) or sI/R (Figure 5A and 5B). In contrast, myocytes isolated from ATF6 KO mouse hearts showed no induction of GRP78 in response to TM (Online Figure IXC and IXD) or sI/R (Figure 5C and D). Moreover, compared with myocytes from WT mouse hearts, myocytes from ATF6 KO mouse hearts exhibited greater death in response to sI/R (Figure 5E). Thus, the deleterious effects of ATF6 deletion on ATF6 target gene induction by TM or sI/R, as well as sI/R-mediated cell death, were observed in ATF6 KO mouse hearts in vivo and ex vivo, as well as in myocytes isolated from ATF6 KO mouse hearts.

Because ATF6 reduced ROS levels and protected cardiac myocytes and hearts against oxidative stress, we examined whether ATF6 overexpression in NRVM affected the levels of typical oxidative stress response genes. An initial survey of expression levels of several typical antioxidant genes, that is, superoxide dismutase 1 and 2, glutathione peroxidase 1, 3, and 4, and peroxiredoxin 1 to 4 and 6 (Prdx1–4/6), showed that compared with control, ATF6 had a small effect on the expression of any of these genes (Figure 6A). Accordingly, a wider range of oxidative stress response genes was assessed using a polymerase chain reaction gene array. Among the 84 genes represented in the array, ATF6 significantly changed the levels of 17 genes; 11 genes were increased by ATF6, including catalase, Prdx5, and Vimp (Figure 6B, red), which encode antioxidant proteins, while 6 genes were decreased by ATF6 (Figure 6B, green), most of which respond to oxidative stress, but do not encode antioxidants. Details of the proteins encoded by the genes shown in Figure 6B can be found in Online Table II. Polymerase chain reaction was used to examine the

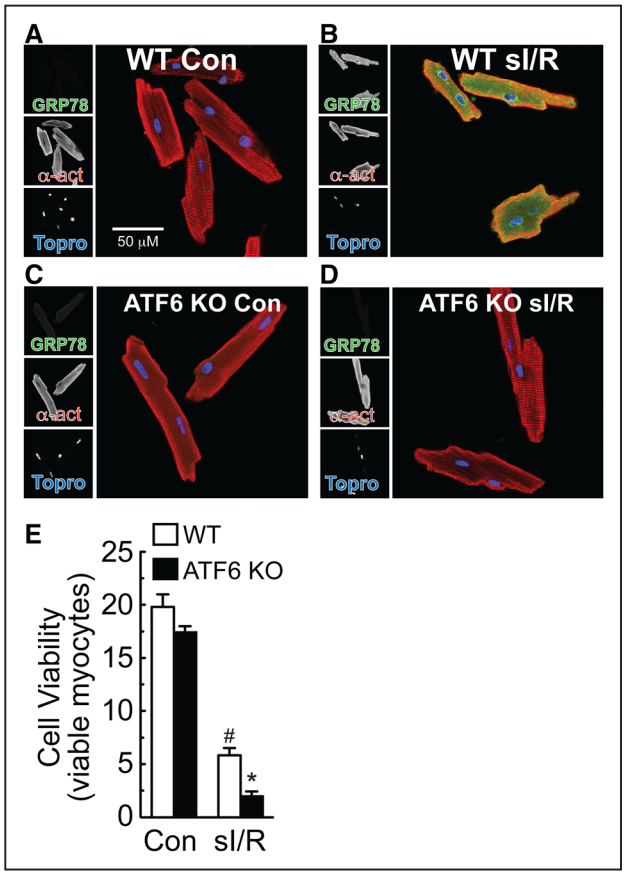

Figure 5. Effect of ATF6 deletion on GRP78 expression and cell viability of isolated adult mouse ventricular myocytes. **A–D,** Myocytes were isolated from adult wild-type (WT) or ATF6 knockout (KO) mice, subjected to sI/R, then fixed and examined by immunocytofluorescence (ICF) for GRP78 (green), α-actinin (red), or TOPRO (blue). **E,** Myocytes were isolated from adult WT or ATF6 KO mice, then subjected to sI/R followed by determination of cell viability using calcein blue AM staining. n=3 cultures for each treatment; shown is a representative experiment of 3 independent experiments, *#$P \leq 0.05$, different than all other groups by analysis of variance (ANOVA). ATF6 indicates activating transcription factor 6 alpha; GRP78, glucose-regulated protein 78 kDa; and sI/R, simulated ischemia/reperfusion.

expression of several key genes in the array on which ATF6 had the most robust induction effects, Cat, Prdx5, and Vimp. Form 1 of ATF6 was the strongest inducer of all 3 genes, with much less induction being observed for forms 2 and 3 (Figure 6C). These results suggested that ATF6 might directly transcriptionally induce these genes.

Because catalase is known to decrease I/R damage in the heart,[31] we probed deeper into the mechanism by which ATF6 mediated the induction of catalase, which has not been studied before. Immunoblots of NRVM treated with the 3 forms of ATF6 showed that catalase protein levels were increased most by form 1, followed by form 2 and then not at all by form 3 (Figure 6D), consistent with the effects of these forms of ATF6 on catalase mRNA (Figure 6C). Moreover, when mice were injected with a recombinant adeno-associated virus 9 that expresses form 1 of ATF6 in cardiac myocytes (Figure 6E; FLAG), immunoblots of heart extracts showed that catalase was robustly induced by ATF6 overexpression in the mouse heart, in vivo (Figure 6E, catalase). As a control, we showed that adeno-associated virus 9-ATF6 also induced the known ATF6 target gene, GRP78 (Figure 6E, GRP78). Knocking down catalase in NRVM with siRNA (Figure 6F) decreased cell viability and increased ROS generation in response to sI/R (Figure 6G and 6H). Quantitative reverse transcriptase polymerase chain reaction of mouse hearts subjected to I/R showed that compared with WT mouse hearts, catalase was about half in ATF6 KO mouse hearts (Figure 6I). Although myocytes isolated from WT mouse hearts exhibited a strong induction of catalase by TM (Online Figure XA and XB) or sI/R (Figure 7A and 7B), catalase did not increase in myocytes isolated from ATF6 KO mouse hearts treated with either TM (Online Figure XC and XD) or sI/R (Figure 7C and 7D). Immunocytofluorescence of mouse heart tissue sections showed that catalase increased in the hearts of WT mouse hearts subjected to I/R, in vivo, but not in ATF6 KO mouse hearts (Online Figure XIA through XID). Immunoblots verified the impaired induction of catalase in the hearts of ATF6 KO mice subjected to I/R, in vivo (Online Figure XIE and XIF). In NRVM, catalase siRNA decreased the beneficial effects of ATF6 form 1, indicating that catalase is a major contributor of ATF6-mediated protection from I/R induced cell death in cardiac myocytes (Figure 7E). Moreover, the increased susceptibility of ATF6 KO myocytes to death from I/R was rescued by treating them with a cell-permeable form of catalase, PEG catalase, as previously described,[32] after which there was no difference in viability between myocytes from WT and ATF6 KO mouse hearts (Figure 7F). Treatment of mice with PEG catalase in vivo, as previously described,[33] resulted in a similar rescue of left ventricular developed pressure in ATF6 KO mouse hearts subjected to ex vivo I/R, such that the performance of WT and ATF6 KO mouse hearts was indistinguishable (Figure 7G). This catalase-mediated rescue was also seen when LDH release and infarct size were measured in WT versus ATF6 KO mouse hearts subjected to ex vivo I/R (Figure 7H and 7I). Moreover, the PEG catalase rescue effect was recapitulated by adeno-associated virus 9–mediated ATF6 overexpression in ATF6 KO mouse hearts (Figure 7J).

To further examine the mechanism by which ATF6 induces catalase, the 5′-flanking sequence of the rat Cat gene was scanned for a DNA sequence that might bind ATF6, that is an ER stress response element (ERSE). Two such elements were found within 1000 nucleotides 5′ of the Cat mRNA start site; we named these ERSE-1 (−194 to −184) and ERSE-2 (−979 to −962). To examine whether the rat Cat 5′-flanking sequences conferred transcriptional induction in response to ATF6, truncated versions of the rat Cat 5′-flanking sequence were cloned in front of firefly luciferase, and the abilities of cotransfected ATF6 form 1 to induce luciferase were examined in NRVM. Truncating from −1161 to −689 and to −410, which removed ERSE-2, had little effect on ATF6 induction (Figure 8A, constructs 1–3). However, a truncated form of rat Cat that removed ERSE-1 resulted in a significant decrease in ATF6-mediated luciferase induction (Figure 8A, construct 4). Next, ERSE-1 and ERSE-2 were mutated in ways predicted to inhibit ATF6 binding (Figure 8B, M1 and M2). When these reporters were cotransfected with the various forms of ATF6 into NRVM, the mutation in ERSE-2, that is, M2, moderately decreased Cat

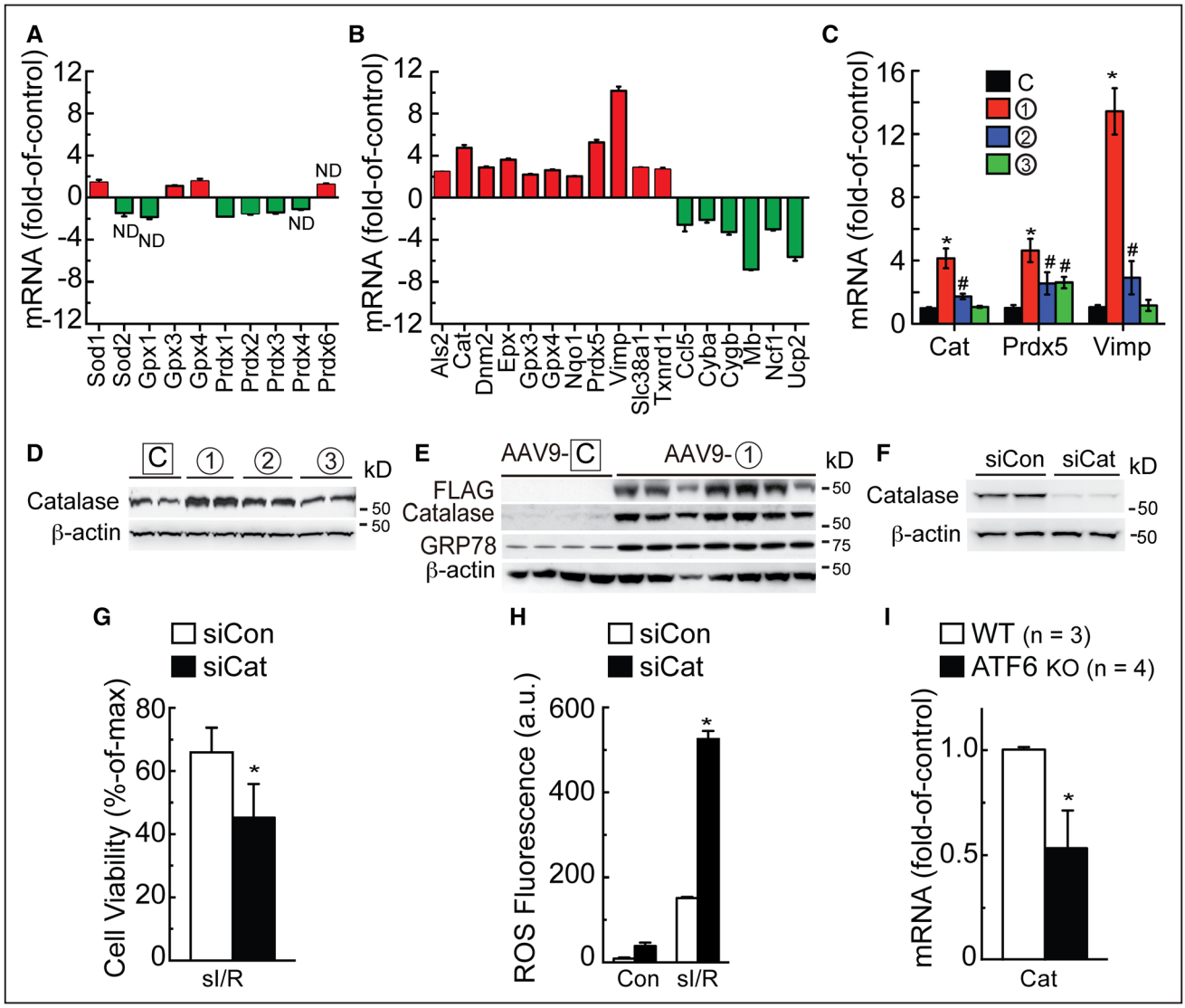

Figure 6. Analysis of oxidative stress gene expression. A and B, NRVM were infected with AdV-Con or AdV-ATF6 (form 1), and then RNA was subjected to quantitative reverse transcriptase polymerase chain reaction (qRT-PCR) for the genes shown (**A**) or analyzed with an oxidative stress gene array (**B**). Shown are only genes that were increased (red) or decreased (green) by ATF6. In **A** and **B**, all values were $P \leq 0.05$, different than control by *t* test, unless marked ND (no difference). **C and D,** NRVM were infected with the AdV-ATF6 shown; then RNA was isolated and analyzed for catalase (Cat), peroxiredoxin 5 (Prdx5), and Vimp mRNA by qRT-PCR (**C**), *#$P \leq 0.05$, different than all other values for each target gene, and protein was analyzed for catalase levels by immunoblotting (**D**). **E,** Wild-type (WT) mice were injected with adeno-associated virus 9 (AAV9)-control or AAV9-CMV-FLAG-ATF6 form 1. Two weeks later, mice were euthanized, and hearts were analyzed for FLAG-ATF6, catalase, GRP78, and β-actin by immunoblotting. **F,** NRVM were transfected with siCon or siCat RNAs; 48 h later, culture extracts were examined for catalase and β-actin. **G and H,** NRVM were transfected with siCon or siCat RNA, subjected to sI/R, then analyzed for cell viability by calcein blue AM staining (**G**) or for ROS by Amplex Red (**H**). **I,** Following I/R, WT (n=3), and ATF6 knockout (KO; n=4), mouse heart extracts were analyzed for Cat mRNA levels, normalized to β-actin mRNA by qRT-PCR. *$P \leq 0.05$, different from siCon (**G** and **H**) or WT (**I**) by *t* test. Adv indicates adenovirus; ATF6, activating transcription factor 6 alpha; GRP78, glucose-regulated protein 78 kDa; I/R, ischemia/reperfusion; NRVM, neonatal rat ventricular myocytes; ROS, reactive oxygen species; and sI/R, simulated ischemia/reperfusion.

promoter activity, while the mutation in ERSE-1, that is, M1, or in both ERSE-1 and ERSE-2, that is, M1/M2, showed greater reductions of ATF6-mediated transcriptional induction (Figure 8C). Finally, a chromatin immunoprecipitation experiment showed that form 1 of ATF6 was able to bind to either ERSE-1 or ERSE-2 in cardiac myocytes (Figure 8D). Thus, activated ATF6 can bind to putative ERSEs in the rat Cat gene regulatory region and confer transcriptional induction, demonstrating one mechanism by which ATF6 could protect cardiac myocytes from oxidative stress during I/R.

Discussion

ATF6 Links the ER Stress Response and the Oxidative Stress Response

This study provides evidence supporting a newly described role for ATF6 as a molecular link between the ER stress and oxidative stress gene programs. Initially, we thought that this role for ATF6 fit well with a potential connection between ER stress and oxidative stress involving protein disulfide bond formation. Protein disulfide bond formation, which

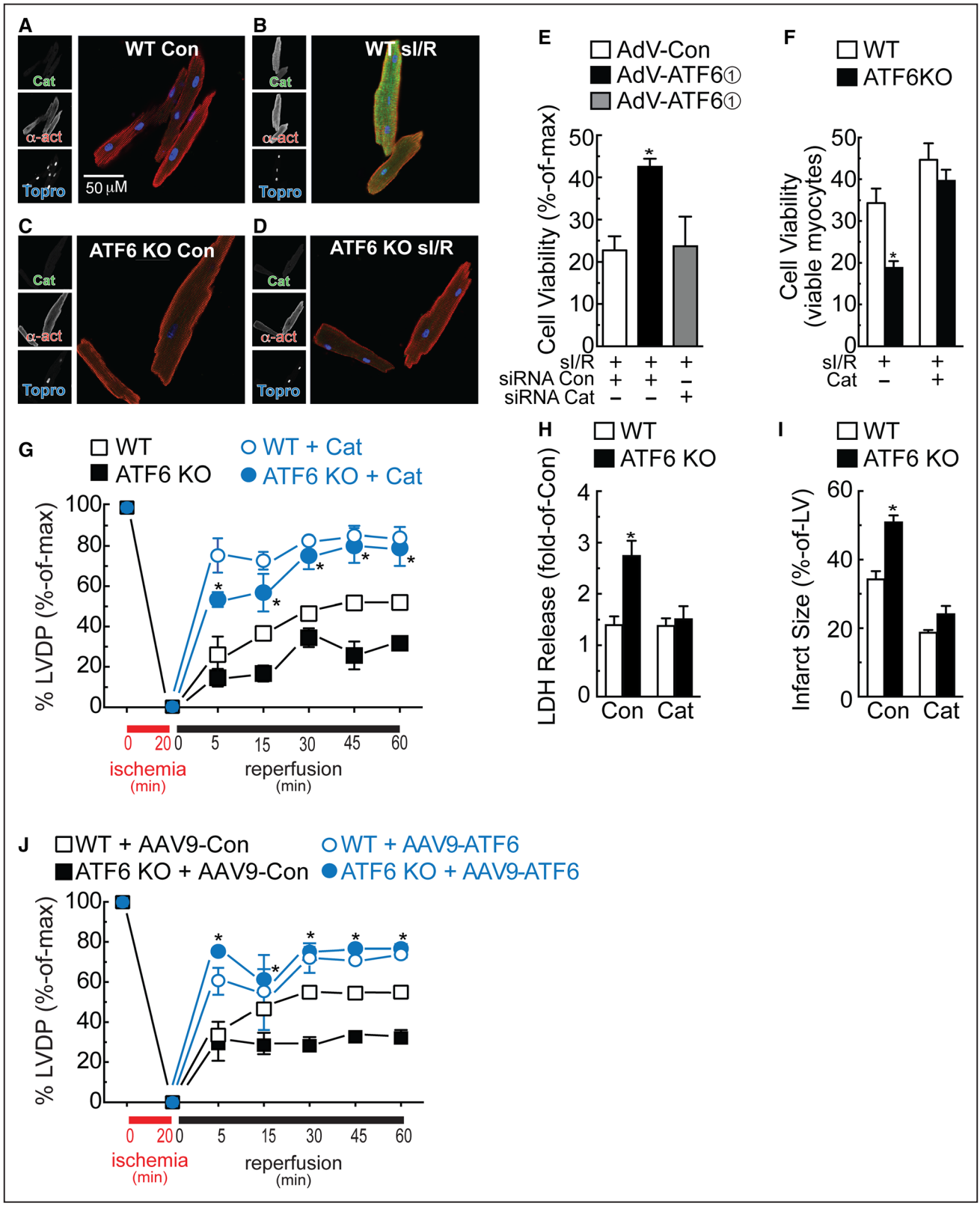

Figure 7. Effects of ATF6 deletion on catalase. A–D, Myocytes were isolated from adult wild-type (WT; **A** and **B**) or ATF6 knockout (KO; **C** and **D**) mice, subjected to sI/R, then fixed and examined by immunocytofluorescence (ICF) for catalase (green), α-actinin (red), or TOPRO (blue). **E,** NRVM were treated with siCon or siCat RNAs, as well as infection with the AdVs shown, then subjected to sI/R followed by determination of cell viability by calcein blue AM staining. *$P \leq 0.05$ different from all other values by analysis of variance (ANOVA). **F,** Myocytes isolated from WT or ATF6 KO mouse hearts were treated with vehicle or PEG catalase, followed by sI/R; the viability was determined by calcein blue AM staining. *$P \leq 0.05$ different from WT by *t* test. **G-I,** Mice were injected with vehicle or PEG Cat for 16 h, then hearts were subjected to ex vivo I/R and left ventricular developed pressure (LVDP), (*Continued*)

Figure 7. Continued LDH (lactate dehydrogenase) release, and infarct size were measured. In **G**, *$P \leq 0.001$, different from WT vehicle or ATF6 KO vehicle at a given reperfusion time by 2-way ANOVA. In **H** and **I**, *$P \leq 0.001$, different from WT Con, by *t* test. **J**, Mice were injected with adeno-associated virus 9 (AAV9-Con) or AAV9-CMV-FLAG-ATF6 form 1 (AAV9-ATF6) for 2 d, then hearts were subjected to ex vivo I/R, and LVDP was measured. *$P \leq 0.001$ different from WT AAV9-Con or ATF6 KO AAV9-Con at a given reperfusion time by 2-way ANOVA. Adv indicates adenovirus; ATF6, activating transcription factor 6 alpha; I/R, ischemia/reperfusion; NRVM, neonatal rat ventricular myocytes; I/R, ischemia/reperfusion; and sI/R, simulated ischemia/reperfusion.

takes place only in the ER, requires oxygen to fuel the redox couple between ER oxidoreductase 1 and the final enzyme involved in protein disulfide bond formation, protein disulfide isomerase[19,34,35] (Figure 8E). This ER redox system results in the conversion of molecular oxygen to H_2O_2, the latter of which contributes to total cellular ROS, although a small amount compared with the ROS generated by mitochondria.[36] There are 3 ER proteins thought to be responsible for neutralizing the H_2O_2 generated during protein disulfide bond formation in the ER; Prx4, and glutathione perioxidases 7, and 8 (GPx7/8).[34] Accordingly, when we first discovered that ATF6 had antioxidant activity, because ATF6 induces ER proteins, we thought that ATF6 most likely exerted its antioxidant effects by inducing antioxidant proteins that reside in the ER, such as Prx4 or GPx7/8. However, our results showed that these genes were minimally affected by ATF6 and that ATF6 had more robust effects on expression of 11 other genes, all but one of which encode antioxidant proteins that reside outside of the ER (Figure 6; Online Table II). Thus, ATF6 can have widespread effects on antioxidant protein expression, even outside the ER, which increases the scope of the functional impact of ATF6 well beyond improving ER protein folding. It might be of clinical relevance to acutely activate ATF6 during reperfusion, in vivo, but this would likely require the development of new methods that do not depend on ATF6 overexpression. Although many of the antioxidant proteins induced by ATF6 may contribute in some way to reducing myocardial damage during I/R, we focused the mechanistic aspects of this study on catalase because of its ability to neutralize large quantities of ROS generated in various cellular locations and because it has not previously been shown to be induced in an ATF6- and ER stress-dependent manner in any cell or tissue.

Catalase Is an Example of How ATF6 Regulates Antioxidant Protein Expression

Catalase is a 527 amino acid protein (rat) that resides mainly in peroxisomes. Peroxisomes generate and use H_2O_2 for oxidative purposes, including peroxidative detoxification and β-oxidation of fatty acids. Catalase is an important component of peroxisomes because it neutralizes H_2O_2 that remains after the required peroxidative reactions have taken place. Catalase can also oxidize peroxynitrate, nitric oxide, and organic peroxides. In addition to peroxisomes, catalase has also been found in the cytosol and in cardiac mitochondria; however, it has not been found in the ER. Moreover, it has been shown that in the heart, catalase overexpression in cardiac myocytes decreases I/R injury by reducing ROS levels.[31]

Here, we showed that, in cardiac myocytes, ischemia, which impairs ER protein disulfide bond formation and increases misfolded proteins, activates ATF6, which binds to specific elements in the regulatory regions of the catalase gene and increases catalase transcription. We also showed that ATF6 can increase expression of other antioxidant proteins, supporting the hypothesis that together with catalase, these antioxidants decrease ROS and moderate myocardial damage during reperfusion (Figure 8F). In further support of this hypothesis was our finding that compared with WT mouse hearts, the induction of catalase during I/R was impaired in ATF6KO mouse hearts. To the best of our knowledge, this is the first demonstration that catalase is induced in the heart by I/R in an ATF6-dependent manner. Because we showed that ATF6 also induced 2 other antioxidant genes encoding proteins residing outside the ER, it seems that during ER stress induced by ischemia, ATF6 is likely to be a direct transcriptional inducer of numerous antioxidant genes.

Catalase Is an ATF6-Inducible ER Stress Response Gene

Previous studies, mostly in noncardiac myocytes, have shown that catalase expression is regulated by the transcription factors Sp1, NF-Y, and Foxo3a.[37] However, there have been no studies examining whether ATF6 can regulate catalase transcription. Here, we showed that there are 2 sites in the catalase regulatory region to which ATF6 can bind, ERSE-1 and ERSE-2. Mutating ERSE-2 had less of an effect on catalase promoter activity than mutating ERSE-1, suggesting that ERSE-1, which lies proximal to the catalase promoter, is the major site through which ATF6 confers transcriptional induction in cardiac myocytes (Figure 8A–8D). Moreover, because catalase is induced by the prototypical ER stressor, TM, and by the pathological ER stressor I/R, and because the ER stress transcription factor, ATF6, binds to and induces catalase transcription, we posit that catalase should be categorized as an ER stress response gene. Consistent with the identification of catalase as an ER stress response gene is the apparent reduction of its expression as a function of development in the heart. We previously showed that the expression of numerous canonical ER stress response genes was much higher in neonatal rat cardiac myocytes than in adult rat cardiac myocytes.[38] The same seems to be true for catalase; here, immunoblotting showed higher levels of basal catalase in NRVM compared with adult mouse hearts (Figures 6D and 6E). Therefore, like other ER stress response genes, catalase expression seems to be relatively low in the adult heart, compared with the neonatal heart. This is underscored further by our finding that the ATF6 dependence of catalase expression was evident when adult mouse cardiac myocytes isolated from WT and ATF6 KO mice were treated with TM or sI/R and then immunostained for catalase (Figure 7; Online Figure X).

Global Effects of ATF6 on Antioxidant Protein Expression

The antioxidant genes that were induced the most by ATF6 in this study were catalase, Prdx5, and Vimp. ATF6-mediated induction of these genes was validated using the 3 forms of ATF6;

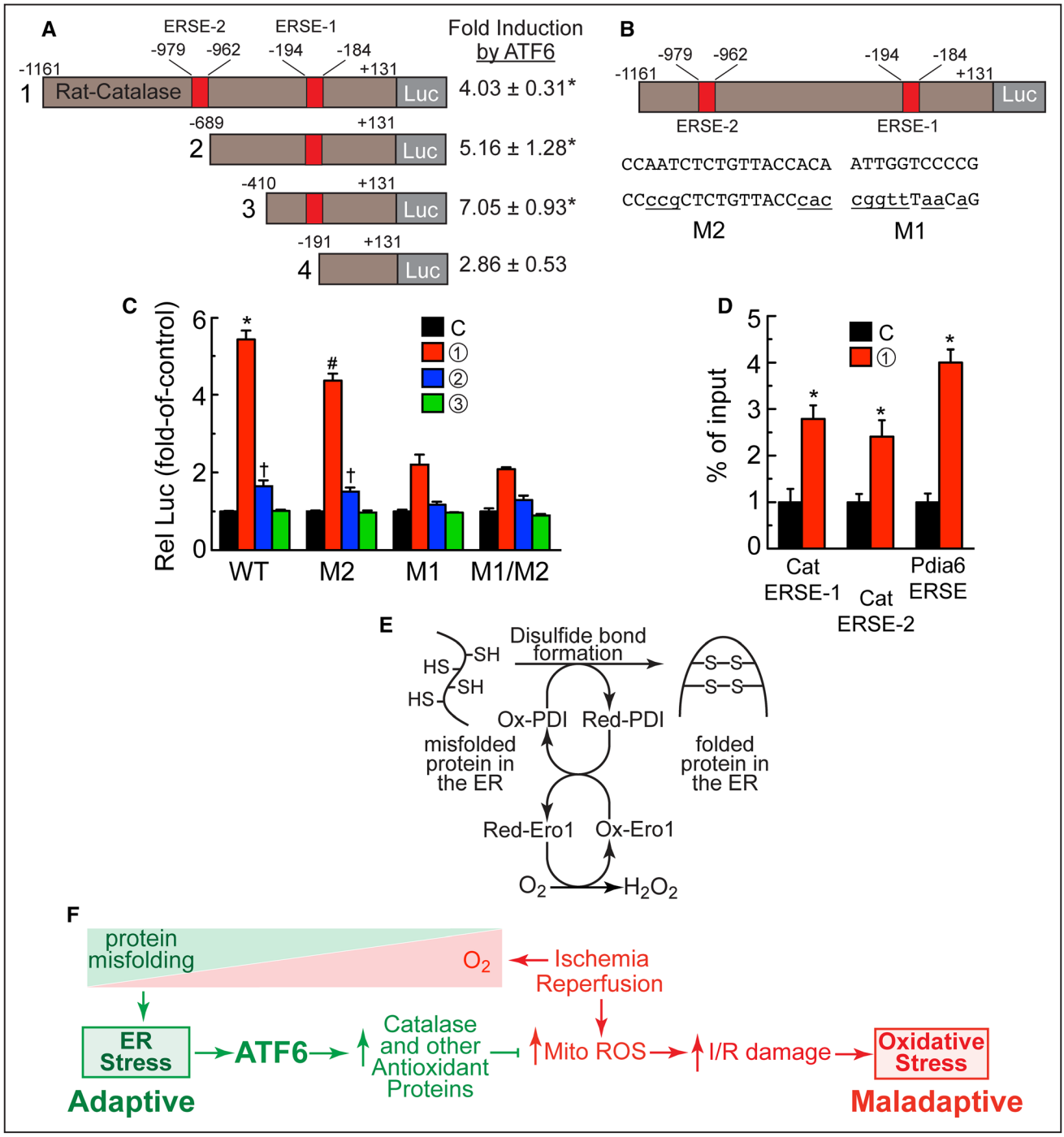

Figure 8. Effects of ATF6 on the catalase promoter. A, Truncations of the catalase 5′-flanking sequence driving luciferase, as shown (**left**), that is, rat-cat(−1161/+131)-Luc, rat-cat(−689/+131)-Luc, rat-cat(−410/+131)-Luc, and rat-cat(−191/+131)-Luc, were transfected into NRVM, which were then infected with AdV encoding form 1 of ATF6 or with a control AdV. Luciferase enzyme activity in AdV-ATF6-infected cells was normalized to luciferase enzyme activity in AdV-Con-infected cells to determine the fold induction by ATF6 (**right**), **P*≤0.05 different from control by *t* test. **B,** Diagram of the locations of ERSE-2 and 1 in the catalase 5′-flanking region, their sequences (upper case), and the mutations to those sequences (lower case). **C,** NRVM were transfected with plasmids encoding rat-cat(−1161/+131)-Luc WT, M2, M1, or M1/M2 and then infected with the ATF6-expressing AdV, as shown; then, 48 h later, luciferase levels were measured in extracts, *#†*P*≤0.05, different than other values in WT or M2 by analysis of variance (ANOVA). **D,** NRVM were infected with AdV encoding control or FLAG-ATF6 (form 1), and then ATF6 binding to endogenous ERSE-1 or ERSE-2, as well as to the endogenous Pdia6 ERSE, previously studied and used here as a control, was examined by ChIP (chromatin immunoprecipitation), **P*≤0.05, different than control by *t* test. **E,** O_2 is required for protein disulfide bond formation and protein folding in the ER. **F,** ATF6 links the ER stress response with the oxidative stress response. As O_2 decreases during ischemia (red triangle), protein misfolding increases (green triangle), leading to adaptive ER stress, ATF6 activation and induction of catalase and other antioxidant proteins that decrease ROS generated in the mitochondria during reperfusion. Adv indicates adenovirus; ATF6, activating transcription factor 6 alpha; ER, endoplasmic reticulum; NRVM, neonatal rat ventricular myocytes; and ROS, reactive oxygen species.

each gene was induced with a profile consistent with the direct effects of ATF6 on transcription (Figure 6C). Like catalase, Prdx5 is not located in the ER lumen; however, it is unusual among other isoforms of Prdx in that it has been found in several cellular locations including mitochondria, peroxisomes, cytosol, and nucleus[39] (Online Table II). Prdx5 is a 213 amino acid protein (rat) that catalyzes the glutathione-mediated reduction of potentially damaging peroxides, providing a new mechanism by which the ATF6 branch of the ER stress response could contribute to decreasing ROS during myocardial reperfusion.

Vimp is a 189 amino acid ER-transmembrane protein (rat) configured with most of its structure, including its catalytic domain on the cytosolic face of the ER.[40] Vimp, also known as SelS, is believed to interact with Hrd1 and other ER stress, ATF6-regulated ER-transmembrane proteins that are involved in ER-associated degradation, a process by which terminally misfolded proteins in the ER are degraded to mitigate their toxic effects. Vimp is one of only 24 selenoprotein genes in the mouse genome; in general, selenoproteins are known for their antioxidant roles as ROS scavengers.[41] However, the functions of selenoproteins and, in particular, Vimp, have not been studied in the heart. It is interesting to note that 5 of the 11 ATF6-inducible oxidative stress response genes identified in this study are selenoproteins. This is the first demonstration in any cell or tissue-type that ATF6 has a global effect on selenoprotein expression, which provides even further linkage between the ATF6 branch of the ER stress response and the oxidative stress response.

In summary, previous studies showed that ectopic expression of activated ATF6 can decrease I/R damage in the heart.[16] However, neither the mechanism of this effect nor whether endogenous ATF6 plays a role in myocardial I/R damage had been examined. Here, we determined functions for endogenous ATF6 in the heart and found evidence of a previously unappreciated role for ATF6 as an inducer of antioxidant genes, which establishes a mechanistic link by which ATF6 can decrease myocardial I/R damage (Figure 8F).

Sources of Funding

J.K. Jin was supported by an American Heart Association, Postdoctoral Fellowship 16POST27510010. S. Doroudgar was supported by an Excellence Grant from the German Centre for Cardiovascular Research (DZHK). C.C. Glembotski was supported by National Institutes of Health (NIH) grants R01 HL75573, R01 HL104535, R01 HL127439, and P01 HL085577. R.J. Kaufman was supported by NIH/NCI grants R37DK042394, R01DK103185, R24DK110973, R01CA198103, and the Sanford Burnham Prebys NCI Cancer Center Grant P30 CA030199.

Disclosures

None.

References

1. Balch WE, Morimoto RI, Dillin A, Kelly JW. Adapting proteostasis for disease intervention. *Science*. 2008;319:916–919. doi: 10.1126/science.1141448.
2. Glembotski CC. Roles for the sarco-/endoplasmic reticulum in cardiac myocyte contraction, protein synthesis, and protein quality control. *Physiology (Bethesda)*. 2012;27:343–350. doi: 10.1152/physiol.00034.2012.
3. Gidalevitz T, Stevens F, Argon Y. Orchestration of secretory protein folding by ER chaperones. *Biochim Biophys Acta*. 2013;1833:2410–2424. doi: 10.1016/j.bbamcr.2013.03.007.
4. Amm I, Sommer T, Wolf DH. Protein quality control and elimination of protein waste: the role of the ubiquitin-proteasome system. *Biochim Biophys Acta*. 2014;1843:182–196. doi: 10.1016/j.bbamcr.2013.06.031.
5. Guerriero CJ, Brodsky JL. The delicate balance between secreted protein folding and endoplasmic reticulum-associated degradation in human physiology. *Physiol Rev*. 2012;92:537–576. doi: 10.1152/physrev.00027.2011.
6. Dickhout JG, Carlisle RE, Austin RC. Interrelationship between cardiac hypertrophy, heart failure, and chronic kidney disease: endoplasmic reticulum stress as a mediator of pathogenesis. *Circ Res*. 2011;108:629–642. doi: 10.1161/CIRCRESAHA.110.226803.
7. Minamino T, Komuro I, Kitakaze M. Endoplasmic reticulum stress as a therapeutic target in cardiovascular disease. *Circ Res*. 2010;107:1071–1082. doi: 10.1161/CIRCRESAHA.110.227819.
8. Doroudgar S, Glembotski CC. New concepts of endoplasmic reticulum function in the heart: programmed to conserve. *J Mol Cell Cardiol*. 2013;55:85–91. doi: 10.1016/j.yjmcc.2012.10.006.
9. Millott R, Dudek E, Michalak M. The endoplasmic reticulum in cardiovascular health and disease. *Can J Physiol Pharmacol*. 2012;90:1209–1217. doi: 10.1139/y2012-058.
10. Olzmann JA, Kopito RR, Christianson JC. The mammalian endoplasmic reticulum-associated degradation system. *Cold Spring Harb Perspect Biol*. 2012;5:a013185. doi: 10.1101/cshperspect.a013185.
11. Malhotra JD, Kaufman RJ. The endoplasmic reticulum and the unfolded protein response. *Semin Cell Dev Biol*. 2007;18:716–731. doi: 10.1016/j.semcdb.2007.09.003.
12. Glembotski CC. Endoplasmic reticulum stress in the heart. *Circ Res*. 2007;101:975–984. doi: 10.1161/CIRCRESAHA.107.161273.
13. Walter P, Ron D. The unfolded protein response: from stress pathway to homeostatic regulation. *Science*. 2011;334:1081–1086. doi: 10.1126/science.1209038.
14. Zhu C, Johansen FE, Prywes R. Interaction of ATF6 and serum response factor. *Mol Cell Biol*. 1997;17:4957–4966.
15. Haze K, Yoshida H, Yanagi H, Yura T, Mori K. Mammalian transcription factor ATF6 is synthesized as a transmembrane protein and activated by proteolysis in response to endoplasmic reticulum stress. *Mol Biol Cell*. 1999;10:3787–3799.
16. Martindale JJ, Fernandez R, Thuerauf D, Whittaker R, Gude N, Sussman MA, Glembotski CC. Endoplasmic reticulum stress gene induction and protection from ischemia/reperfusion injury in the hearts of transgenic mice with a tamoxifen-regulated form of ATF6. *Circ Res*. 2006;98:1186–1193. doi: 10.1161/01.RES.0000220643.65941.8d.
17. Belmont PJ, Tadimalla A, Chen WJ, Martindale JJ, Thuerauf DJ, Marcinko M, Gude N, Sussman MA, Glembotski CC. Coordination of growth and endoplasmic reticulum stress signaling by regulator of calcineurin 1 (RCAN1), a novel ATF6-inducible gene. *J Biol Chem*. 2008;283:14012–14021. doi: 10.1074/jbc.M709776200.
18. Yamamoto K, Sato T, Matsui T, Sato M, Okada T, Yoshida H, Harada A, Mori K. Transcriptional induction of mammalian ER quality control proteins is mediated by single or combined action of ATF6alpha and XBP1. *Dev Cell*. 2007;13:365–376. doi: 10.1016/j.devcel.2007.07.018.
19. Cao SS, Kaufman RJ. Endoplasmic reticulum stress and oxidative stress in cell fate decision and human disease. *Antioxid Redox Signal*. 2014;21:396–413. doi: 10.1089/ars.2014.5851.
20. Granger DN, Kvietys PR. Reperfusion injury and reactive oxygen species: The evolution of a concept. *Redox Biol*. 2015;6:524–551. doi: 10.1016/j.redox.2015.08.020.
21. Wu J, Rutkowski DT, Dubois M, Swathirajan J, Saunders T, Wang J, Song B, Yau GD, Kaufman RJ. ATF6alpha optimizes long-term endoplasmic reticulum function to protect cells from chronic stress. *Dev Cell*. 2007;13:351–364. doi: 10.1016/j.devcel.2007.07.005.
22. Yoshida H, Okada T, Haze K, Yanagi H, Yura T, Negishi M, Mori K. ATF6 activated by proteolysis binds in the presence of NF-Y (CBF) directly to the cis-acting element responsible for the mammalian unfolded protein response. *Mol Cell Biol*. 2000;20:6755–6767.
23. Thuerauf DJ, Morrison LE, Hoover H, Glembotski CC. Coordination of ATF6-mediated transcription and ATF6 degradation by a domain that is shared with the viral transcription factor, VP16. *J Biol Chem*. 2002;277:20734–20739. doi: 10.1074/jbc.M201749200.
24. Thuerauf DJ, Morrison L, Glembotski CC. Opposing roles for ATF6alpha and ATF6beta in endoplasmic reticulum stress response gene induction. *J Biol Chem*. 2004;279:21078–21084. doi: 10.1074/jbc.M400713200.

25. Marshall KD, Edwards MA, Krenz M, Davis JW, Baines CP. Proteomic mapping of proteins released during necrosis and apoptosis from cultured neonatal cardiac myocytes. *Am J Physiol Cell Physiol*. 2014;306:C639–C647. doi: 10.1152/ajpcell.00167.2013.
26. Siman R, McIntosh TK, Soltesz KM, Chen Z, Neumar RW, Roberts VL. Proteins released from degenerating neurons are surrogate markers for acute brain damage. *Neurobiol Dis*. 2004;16:311–320. doi: 10.1016/j.nbd.2004.03.016.
27. van Wijk SJ, Hageman GJ. Poly(ADP-ribose) polymerase-1 mediated caspase-independent cell death after ischemia/reperfusion. *Free Radic Biol Med*. 2005;39:81–90. doi: 10.1016/j.freeradbiomed.2005.03.021.
28. Griendling KK, Touyz RM, Zweier JL, Dikalov S, Chilian W, Chen YR, Harrison DG, Bhatnagar A; American Heart Association Council on Basic Cardiovascular Sciences. Measurement of reactive oxygen species, reactive nitrogen species, and redox-dependent signaling in the cardiovascular system: a scientific statement from the American Heart Association. *Circ Res*. 2016;119:e39–e75. doi: 10.1161/RES.0000000000000110.
29. Santos CX, Raza S, Shah AM. Redox signaling in the cardiomyocyte: from physiology to failure. *Int J Biochem Cell Biol*. 2016;74:145–151. doi: 10.1016/j.biocel.2016.03.002.
30. Pompella A, Maellaro E, Casini AF, Ferrali M, Ciccoli L, Comporti M. Measurement of lipid peroxidation in vivo: a comparison of different procedures. *Lipids*. 1987;22:206–211.
31. Li G, Chen Y, Saari JT, Kang YJ. Catalase-overexpressing transgenic mouse heart is resistant to ischemia-reperfusion injury. *Am J Physiol*. 1997;273:H1090–H1095.
32. Nakagami H, Takemoto M, Liao JK. NADPH oxidase-derived superoxide anion mediates angiotensin II-induced cardiac hypertrophy. *J Mol Cell Cardiol*. 2003;35:851–859.
33. Schröder K, Zhang M, Benkhoff S, Mieth A, Pliquett R, Kosowski J, Kruse C, Luedike P, Michaelis UR, Weissmann N, Dimmeler S, Shah AM, Brandes RP. Nox4 is a protective reactive oxygen species generating vascular NADPH oxidase. *Circ Res*. 2012;110:1217–1225. doi: 10.1161/CIRCRESAHA.112.267054.
34. Delaunay-Moisan A, Appenzeller-Herzog C. The antioxidant machinery of the endoplasmic reticulum: Protection and signaling. *Free Radic Biol Med*. 2015;83:341–351. doi: 10.1016/j.freeradbiomed.2015.02.019.
35. Higa A, Chevet E. Redox signaling loops in the unfolded protein response. *Cell Signal*. 2012;24:1548–1555. doi: 10.1016/j.cellsig.2012.03.011.
36. Tu BP, Weissman JS. Oxidative protein folding in eukaryotes: mechanisms and consequences. *J Cell Biol*. 2004;164:341–346. doi: 10.1083/jcb.200311055.
37. Glorieux C, Zamocky M, Sandoval JM, Verrax J, Calderon PB. Regulation of catalase expression in healthy and cancerous cells. *Free Radic Biol Med*. 2015;87:84–97. doi: 10.1016/j.freeradbiomed.2015.06.017.
38. Doroudgar S, Völkers M, Thuerauf DJ, Khan M, Mohsin S, Respress JL, Wang W, Gude N, Müller OJ, Wehrens XH, Sussman MA, Glembotski CC. Hrd1 and ER-associated protein degradation, ERAD, are critical elements of the adaptive ER stress response in cardiac myocytes. *Circ Res*. 2015;117:536–546. doi: 10.1161/CIRCRESAHA.115.306993.
39. Knoops B, Goemaere J, Van der Eecken V, Declercq JP. Peroxiredoxin 5: structure, mechanism, and function of the mammalian atypical 2-Cys peroxiredoxin. *Antioxid Redox Signal*. 2011;15:817–829. doi: 10.1089/ars.2010.3584.
40. Liu J, Rozovsky S. Membrane-bound selenoproteins. *Antioxid Redox Signal*. 2015;23:795–813. doi: 10.1089/ars.2015.6388.
41. Reeves MA, Hoffmann PR. The human selenoproteome: recent insights into functions and regulation. *Cell Mol Life Sci*. 2009;66:2457–2478. doi: 10.1007/s00018-009-0032-4.

Circulation Research
JOURNAL OF THE AMERICAN HEART ASSOCIATION

ATF6 Decreases Myocardial Ischemia/Reperfusion Damage and Links ER Stress and Oxidative Stress Signaling Pathways in the Heart

Jung-Kang Jin, Erik A. Blackwood, Khalid Azizi, Donna J. Thuerauf, Asal G. Fahem, Christoph Hofmann, Randal J. Kaufman, Shirin Doroudgar and Christopher C. Glembotski

Circ Res. 2017;120:862-875; originally published online December 8, 2016;
doi: 10.1161/CIRCRESAHA.116.310266
Circulation Research is published by the American Heart Association, 7272 Greenville Avenue, Dallas, TX 75231

Print ISSN: 0009-7330. Online ISSN: 1524-4571

Supplemental Material

Detailed Methods

Cultured cardiac myocytes

Neonatal rat ventricular myocytes (NRVM) were isolated by enzymatic digestion of neonatal rat hearts and purified by Percoll density gradient centrifugation, as described[1]. Briefly, NRVM were prepared from 1 to 3 day-old Sprague-Dawley rat hearts using a neonatal cardiomyocyte isolation system (cat# LK003300, Worthington Biochemical Corp, Lakewood, NJ). Isolated cells were counted and collected by centrifugation at 250 xg for 5 min. Forty to 60 million cells were then resuspended in 2 ml of red (with phenol red) 1x ADS buffer (116 mM NaCl, 20 mM HEPES, 769 µM NaH_2PO_4, 5.55 mM glucose, 5.37 mM KCl, 831 µM $MgSO_4$, 0.002% phenol red, pH 7.35 ± 0.5). Stock Percoll was prepared by combining 9 parts of Percoll (cat# 17-0891-02, GE healthcare, Piscataway, NJ) with 1 part of clear (without phenol red) 10x ADS. The stock Percoll was used to make the Percoll gradient for the top (density= 1.059 g/ml; 1 part Percoll stock added to 1.2 parts clear 1x ADS) and bottom (density= 1.082 g/ml; 1 part Percoll stock added to 0.54 parts red 1x ADS) layers. The gradient, consisting of 4 ml top Percoll and 3 ml bottom Percoll, was set in a 15 ml conical tube by pipetting the top Percoll first, and layering the bottom Percoll gently underneath, and the cells (in 2 ml red 1x ADS buffer) were layered on the top. Subsequently, the Percoll gradient was centrifuged at 1500×g for 30 min with no deceleration brake at 4°C. The isolated myocytes, which concentrated in the layer located between the lower red ADS layer and the middle clear ADS layer, were carefully collected and washed twice with 50 ml of 1x ADS, and were then resuspended in plating medium and counted. Following Percoll purification, myocytes were plated at the desired density on plastic culture plates that had been pre-treated with 5 µg/ml fibronectin for one hour. Cultures were then maintained in Dulbecco's modified Eagle's medium (DMEM)/F12 supplemented with 10% fetal calf serum (FCS) and antibiotics (100 units/ml penicillin and 100 µg/ml streptomycin).

Adenovirus

Construction of plasmid vectors encoding FLAG-tagged constitutively active ATF6 [ATF6α(1-373)], called form 1 in this paper, partially active ATF6 [ATF6α(39-373)], i.e. form 2, inactive ATF6 [ATF6α(94-373)], i.e. form 3, and empty vector AdV-control (AdV-Con) has been previously described[2]. The ATF6 vectors were used to generate recombinant adenovirus (AdV) expressing different forms of ATF6 using AdEasy system as previously described[3]. AdV-mito-Hyper containing a mitochondria-targeted Hyper protein was a generous gift from Dr. Junichi Sadoshima (New Jersey Medical School, NJ). Transduction was performed by incubating cultures overnight with the appropriate AdV at a multiplicity of infection of five.

Immunoblotting

NRVM were lysed in RIPA buffer comprising 20 mM Tris-HCl (pH 7.5), 150 mM NaCl, 0.1% SDS, 0.5% deoxycholic acid, 1% Triton X-100, protease inhibitor cocktail (Roche Diagnostics, Indianapolis, IN) and phosphatase inhibitor cocktail (Roche Diagnostics). Mouse heart tissues were homogenized in modified RIPA buffer with 1 % SDS. Lysates were clarified by centrifugation at 15,000 x g for 15 min at 4°C, and the protein concentration was determined using DC protein assay (Bio-Rad, Hercules, CA). Samples usually comprising 40 μg of protein were mixed with Laemmli sample buffer, boiled for 5 min, then subjected to SDS-PAGE followed by transferring onto PVDF membrane for immunoblotting analysis. To detect HMGB1 released from cells as a result of necrosis, 20 μl of culture media were analyzed by SDS-PAGE followed by immunoblotting for HMGB1. For ATF6 antibody validation, antibodies raised against the N-terminal of ATF6 were purchased from Proteintech (1:1000, cat# 24169-1-AP, Rosemont, IL), Abcam (1:1000, cat# ab37149, Cambridge, MA), Novus Biologicals (1:1000, cat# NBP1-40256, Littleton, CO), and Santa Cruz Biotechnology (1:500, cat# sc-14250, Dallas, TX). An antibody raised against the C-terminal of ATF6 was purchased from Signalway (1:1000, cat# 32008, College Park, MD). An anti-KDEL antibody (1:8,000, cat# ADI-SPA-827 , Enzo Life Sciences, Farmingdale, NY) was used to detect GRP94, GRP78 and PDIA6, all of which have C-terminal KDEL sequences that cross-react with this antibody. Other antibodies used included anti-PARP (1:1000, cat# 9542, Cell Signaling, Danvers, MA), anti-catalase (1:1000, cat# ab16731, Abcam), anti-FLAG M2 (1:10,000, cat# F1804, Sigma-Aldrich, St. Louis, MO), anti-HMGB1 (1:1000, cat# ab18256 Abcam), anti-CHOP (1:1000, cat# 5554, Cell Signaling), anti-IRE1 (1:500, cat# sc-390960, Santa Cruz), anti-XBP1s (1:1000, cat# 619502, BioLegend, San Diego, CA), anti-phospho-PERK (1:1000, cat# 3179, Cell Signaling), anti-PERK (1:1000, cat# 3192, Cell Signaling), and anti-β-actin (1:1000, cat# sc-47778, Santa Cruz).

MTT and lactate dehydrogenase (LDH) assays

NRVM were plated in 96-well plates (1.5 x 10^4 cells/well) and treated with tunicamycin (TM) at 40 μg/ml for 48h, or with hydrogen peroxide (H_2O_2) at 37.5 μM for 8h. Dose response experiments were carried out to determine that these were the optimal doses of TM and H_2O_2 for measuring the effects of ATF6 gain- and loss-of-function on cell viability (MTT) and necrosis (medium LDH activity). Cell viability was measured using an MTT assay (Cell Proliferation Kit I, Roche Diagnostics), as previously described[1]. Media samples from H_2O_2-treated NRVM were collected for LDH activity assays, which were done using the CytoTox 96 Non-Radioactive Cytotoxicity Assay (Promega, Madison, WI), according to the manufacturer's instructions.

Isolation of adult mouse cardiac myocytes

Adult mouse ventricular myocytes (AMVM) were isolated essentially as previously described [4, 5]. Briefly, hearts were rapidly cannulated via the ascending aorta, mounted on a perfusion apparatus and retrograde perfused at 3 ml/min for 4 min at 37°C with

heart medium (Joklik Modified Minimum Essential Medium; cat# M-0518, Sigma-Aldrich, supplemented with 10 mM HEPES, 30 mM taurine, 2 mM D-L-carnitine, 20 mM creatine, 5 mM inosine, 5 mM adenosine, and 10 mM butanedione monoxime (BDM), pH 7.36). Collagenase digestion of hearts was performed by perfusing for 13 min with heart medium supplemented with type 2 collagenase (50-60 mg; ~320U/ml, cat# LS004176, Worthington) and 12.5 μM $CaCl_2$. Hearts were removed from the cannula and submerged in 2.5 ml of effluent collected off the heart during the collagenase digestion, and dissociated using forceps. Collagenase was neutralized by adding 2.5 ml of heart medium supplemented with 10% FCS, and the final concentration of $CaCl_2$ was adjusted to 12.5 μM. Cells were dissociated further by gently triturating for 4 min. The cell suspension was then filtered through a 100μm mesh filter and myocytes were allowed to sediment by gravity for 6 min at room temperature. The supernatant containing non-viable cells and non-myocytes was discarded and the remaining myocytes were resuspended in 5 ml of heart medium containing 5% FCS and 37.5 μM $CaCl_2$. The concentration of $CaCl_2$ in this suspension was slowly increased in a careful stepwise manner as follows: Step 1- add 50 μl of 10 mM $CaCl_2$, mix gently, allow to sit for 4 min; Step 2- repeat Step 1; Step 3- add 100 μl of 10 mM $CaCl_2$ and wait 4 min; Step 4- add 80 μl of 100 mM $CaCl_2$ and wait 4 min. Cells were resuspended in plating medium (MEM medium; cat# 12350-039, Thermo Fisher Scientific, Waltham, MA, 1x insulin-transferrin-selenium; cat# 41400-045, Thermo Fisher, 10 mM HEPES, 100 units/ml penicillin and 100 μg/ml streptomycin, 10 mM BDM and 4% FCS). Cells were plated at 5 x 10^4 cells per well in 12-well culture plates coated with laminin (10 μg/ml). After at least 2h, the medium was changed to maintaining medium (MEM medium, 1x insulin-transferrin-selenium, 10 mM HEPES, 1.2 mM $CaCl_2$ and 0.01% bovine serum albumin, 25 μM blebbistatin. Cells were used for experiments 12-18h later.

Simulated ischemia/reperfusion

NRVM or AMVM were subjected to simulated ischemia (sI) or simulated ischemia followed by simulated reperfusion (sI/R), as previously described[6]. Briefly, cells were placed into 12-well plates at 2 x 10^5 cells/well for NRVM, or 5 x 10^4 cells/well for AMVM. For sI of NRVM, medium was replaced with 0.5 ml of glucose-free DMEM containing 2% dialyzed FCS. Cells were incubated at 0.1% O_2 in a hypoxia chamber with an oxygen controller (ProOx P110 oxygen controller, Biospherix, Parish, NY). To simulate reperfusion, medium was replaced with medium containing 17.5 mM glucose and cells were incubated at 21% O_2. In some experiments, 5 mM N-acetyl cysteine (pH 7.5), a ROS scavenger, was added to the reperfusion medium. To examine the effects of sI/R on NRVM viability, cells were incubated in sI for 16h, followed by reperfusion for 24h. To examine the effects of sI/R on ROS generation in NRVM, cells were incubated in sI for 8h, followed by reperfusion for 1h. To examine the effects of sI/R on AMVM viability, cells were incubated in DMEM supplemented with 100 units/ml penicillin, 100 μg/ml streptomycin, and 292 μg/ml glutamine for 3h, followed by reperfusion with maintaining medium for 24h. To examine the effects of catalase on sI/R-mediated death of AMVM, cultures were pre-treated with 100U/mL of PEG (polyethylene glycol)-conjugated-Catalase, PEG-Catalase (Sigma cat# C4963) overnight, then PEG-Catalase was added into sI and sI/R media. Viable AMVM and were identified as calcein blue AM-positive

(Thermo Fisher) and images were obtained using an IX70 fluorescence microscope (Olympus, Melville, NY). Numbers of viable, calcein blue AM-positive cells were counted using ImageJ or Image-Pro Plus software (Medium Cybernetics, Rockville, MD).

Reactive oxygen species (ROS) production

The levels of intracellular ROS were determined with the CellROX Orange fluorescent dye (Thermo Fisher). After sI/R, NRVM were incubated with 5 μM CellROX Orange for 20 min at 37°C, and then washed with PBS. Images were obtained using a fluorescence microscope at a magnification of 20X. Fluorescence intensity (absorbance units) was determined using Image-Pro Plus software. To detect intracellular H_2O_2, NRVM were permeabilized with 40 μM digitonin. The resulting media containing intracellular H_2O_2 were transferred to black 96-well plates. The levels of H_2O_2 were measured using Amplex Red Hydrogen Peroxide/peroxidase Assay Kit (Thermo Fisher) according to manufacturer's instructions. Mitochondrial-specific H_2O_2 production was detected through the expression of mitochondria-specific HyPer protein using AdV mito-Hyper as previously described[7].

Small interfering RNA (siRNA) transfection

Reverse transfection of siRNA duplexes into NRVM using TransMessenger Transfection Reagent (Qiagen, Valencia, CA) has been described previously[1]. Briefly, Percoll-purified NRVM (3 x 10^5 cells) were suspended in medium containing 2% FCS, incubated with 100 nM siRNA and transfection reagent followed by plating in 12-well plates for overnight. Medium was changed the next day. The sequence of siRNA targeting rat ATF6 was 5-GCUCUCUUUGUUGUUGCUUAGUGGA-3, and the sequence targeting rat catalase was 5-GGAACCCAAUAGGAGAUAAACUUAA-3 (cat# CatRSS302058, Stealth siRNA, Thermo Fisher). A non-targeting sequence (cat# 12935300, Thermo Fisher) was used as a control siRNA.

Malondialdehyde assay

Lipid peroxidation was determined by measuring the levels of malondialdehyde (MDA). Briefly, sI/R treated NRVM (6 x 10^5 cells) were scrapped into 0.5 ml of PBS, and sonicated on ice. MDA levels in cell lysates were measured using a TBARS assay kit (Cayman Chemical, Ann Arbor, MI) according to the manufacturer's instructions.

Immunocytofluorescence (ICF)

NRVM- NRVM were plated and on fibronectin-coated glass chamber slides (Nunc Lab-Tek II Chamber Slide) as previously described[1]. After treatment, cells were fixed with -20°C methanol for 10 min, then blocked for 1h with SuperBlock blocking buffer (Thermo Fisher). Slides were then incubated overnight with an anti-ATF6 antibody (1:50, cat# sc-166659, Santa Cruz)[8], and an anti-α-actinin antibody (1:50, cat# GTX103219, GeneTex, Irvine, CA). Slides were subsequently incubated at room temperature for 90

min with the appropriate fluorophore-conjugated a secondary antibody including: Cy3-conjugated anti-mouse IgG (1:100), FITC-conjugated anti-goat IgG (1:100), or FITC-conjugated anti-rabbit IgG (1:100, Jackson ImmunoResearch Laboratories, West Grove, PA). Nuclei were counterstained for 1 min with Topro-3 (1:1000, Thermo Fisher). Images were obtained using laser scanning confocal microscopy on an LSM 710 confocal laser scanning microscope (Carl Zeiss, Oberkochen, Germany).

AMVM- were plated in plating medium at $1.0x10^5$ cells per chamber on laminin-coated 4-chamber glass slides (Falcon). After 3h, the medium was changed to maintaining medium containing 25 μM blebbistatin. After 16h, the medium was replaced with 0.5 ml of medium appropriate for sI/R for the appropriate times (see above), or with medium containing tunicamycin (10 μg/ml) for 24h. After each treatment, AMVM were washed with PBS, fixed for 15 min with 4% paraformaldehyde, followed by permeabilization for 10 min with 0.5% Triton-X. For ATF6 staining, AMVM were fixed for 10 min with -20°C methanol. Slides were blocked for 1h with SuperBlock, and then incubated with primary antibodies for 16h at 4°C. Primary antibodies used for staining AMVM were anti-α-actinin (1:200, cat# A7811, Sigma-Aldrich), anti-GRP78 (C-20, 1:30, cat# SC-1051, Santa Cruz), anti-catalase (1:100, Abcam), and anti-ATF6 (targeting to N-terminus of ATF6, 1:50, cat# sc-14250, Santa Cruz). Slides were incubated with appropriate fluorophore-conjugated secondary antibodies, followed by nuclei counter stain, as described above.

Adult mouse hearts were embedded and sectioned as previously described[11]. Briefly, mice were anesthetized and a catheter was inserted into the abdominal aorta. The aorta was retro-perfused with PBS followed by relaxation buffer containing $CdCl_2$ and KCl, fixed in neutral buffered 10% formalin. After 24h in formalin, the hearts were dehydrated in ethanol and embedded in paraffin. Five-μm sections of paraffin-embedded hearts were heated in antigen retrieval citrate buffer (10mM; pH 6.0). The heart sections were then treated with blocking buffer (Thermo Scientific, cat# 37528) for 1h at room temperature and then incubated with primary antibodies overnight at 4°C. Primary antibodies in this study included: anti-GRP78 (C-20, 1:30, cat# SC-1051, Santa Cruz), anti-catalase (1:50, Abcam), anti-ATF6 (targeting to N-terminus of ATF6, 1:50, cat# sc-14250, Santa Cruz), and anti-tropomyosin (1:200, cat# T9283, Sigma-Aldrich). Slides were incubated with appropriate fluorophore-conjugated secondary antibodies as described above for 90 min at room temperature (all at 1:100 dilutions). Nuclear marker counterstain, TO-PRO-3 (Thermo Fisher; 1:10000), was incubated for 15min at room temperature prior to application of coverslips fixed with Vectashield Hardset (Vector Labs, H1400).

Echocardiography

Echocardiography of WT and ATF6 KO mice was performed using an ultrasound imaging system (Vevo 2100 System, Fujifilm VisualSonics, Toronto, Ontario, Canada) as described[1].

In Vivo ischemia/reperfusion

Myocardial ischemia/reperfusion (I/R) was performed *in vivo* by 30 min of ligation of the left anterior descending coronary artery followed by 24h of reperfusion, as previously described[9]. Following I/R, 1% of Evans Blue was injected apically to determine the area at risk (AAR). Hearts were harvested and 1-mm sections of the hearts were stained with 1% triphenyl tetrazolium chloride (TTC) to measure infarcted area (INF) as previously described[9]. The AAR, INF and left ventricle area (LV) of digital images of heart sections were analyzed using ImageJ software.

Ex vivo ischemia/reperfusion

Mouse hearts were isolated and subjected to global I/R as previously described[10]. Briefly, isolated hearts were mounted onto a Langendorff perfused heart apparatus. Global no-flow ischemia was performed for 20 min followed by reperfusion for 1 h. Left ventricular developed pressure (LVDP) was measured using a pressure sensor balloon and analyzed using Powerlab software (ADInstruments, Colorado Springs, CO).

Intravenous Injections

For AAV9, C57/BL6 mice were anesthetized with 2% isoflurane and then injected via the lateral tail vein with 100 μl of AAV9-control or AAV9-3xFlag-ATF6α(1-373) containing $1x10^{11}$ viral particles, and then hearts were obtained after either 2 weeks for immunoblots **(Fig. 6E)**, or after 2d for *ex vivo* I/R **(Fig. 7J)**. In other experiments, C57/BL6 mice were anesthetized with 2% isoflurane and then injected via the lateral tail vein with 100 μl of 1000u/kg PEG-Catalase (Sigma cat# C4963), or vehicle 16h before hearts were obtained and subjected to *ex vivo* I/R **(Fig. 7G)**.

Quantitative real-time PCR (qRT-PCR)

Total RNA was isolated from NRVM or hearts using Quick-RNA MiniPrep kit (Zymo Research, Irvine, CA) or RNeasy Mini kit (Qiagen), respectively. cDNA synthesis was performed using SuperScript III First-Strand Synthesis System (Thermo Fisher). qRT-PCR was performed using Maxima SYBR Green/ROX qPCR Master Mix in a StepOnePlus RT-PCR System (Thermo Fisher). The following primers were used:

Rat	Forward 5' to 3'	Reverse 5' to 3'
β-Actin	CTTCCTTCCTGGGTATGGAATC	CTGTGTTGGCATAGAGGTCTT
Cat	CTTTGAGGTCACCCACGATATT	GTGGGTTTCTCTTCTGGCTATG
Gpx1	TGAGAAGTGCGAGGTGAATG	CCAGATACCAGGAATGCCTTAG
Gpx3	CATTCGGCCTGGTCATTCT	CAGCGGATGTCATGGATCTT

Gpx4	GCAGGAGCCAGGAAGTAATC	ACGCAGCCGTTCTTATCAA
Prdx1	TGTAGCTCGACTCTGCTGATA	GTCCCAATCCTCCTTGTTTCT
Prdx2	ATGATGAGGGCATCGCTTAC	TCAGGCTCACCGATGTTTAC
Prdx3	CGCTCAGAGGTCTCTTCATTATT	GTACTGGTGCTATGTGCTACTT
Prdx4	GGGAAGGAACAGCTGTGATAA	GATCCAGGCCAAGTGAGTAAA
Prdx5	CAGAGCTGTTCAAGGACAAGA	CCCAAAGAGAGACACCAAAGA
Prdx6	CCTGGAGCAAGGACATCAAT	GGAGTCAACCACTCTGAGAATC
Sod1	TGGGTTCCATGTCCATCAATA	CAATCCCAATCACACCACAAG
Sod2	CTGACCTGCCTTACGACTATG	CTTGCAGTGGGTCCTGATTA
Vimp	GACCTTCTACTTCATCGGTCATC	TCAGAACAGAAATCAGCCCTAC
Mouse		
β-Actin	GACGGCCAGGTCATCACTAT	GTACTTGCGCTCAGGAGGAG
Cat	AACTGGGATCTTGTGGGAAAC	GTGGGTTTCTCTTCTGGCTATG
Grp78	CACGTCCAACCCCGAGAA	ATTCCAAGTGCGTCCGATG
Grp94	TCGTCAGAGCTGATGATGAAGT	GCGTTTAACCCATCCAACTGAAT
Pdia6	TGCCACCATGAATCAGGTTCT	TCGTCCGACCACCATCATAGT

For the RT-PCR array, total RNA was isolated from Ad-Con or Ad-ATF6 form 1 treated NRVM (5 x 10^5 cells) using miRNeasy Mini Kit (Qiagen). Synthesis of cDNA was performed using 500 ng of RNA and RT^2 First Strand Kit (Qiagen). Rat Oxidative Stress RT^2 Profiler PCR Arrays (Qiagen) were performed using RT^2 SYBR Green ROX qPCR Mastermix in a StepOnePlus RT-PCR System according to the manufacturer's instructions.

Adeno-Associated Virus Serotype 9 (AAV9)

AAV9 preparation was carried out essentially as previously described[1]. For generation of recombinant AAV9-control and AAV9-3xFlag-ATF6α(1-373), shuttle vectors for these recombinants were constructed and co-transfected with AAV9 helper, pDG-9 (a gift from Dr. Roger Hajjar) into HEK293T cells to produce virus. Two different expression constructs were prepared; AAV9-CMV-3xFlag-ATF6α(1-373) and AAV9-

CMV_{enh}MLC800-3xFlag-ATF6α(1-373). Similar results were obtained with each vector, except the AAV9-CMV-3xFlag-ATF6α(1-373) results in more robust expression than AAV9-CMV_{enh}MLC800-3xFlag-ATF6α(1-373). Since the recombinant AAV9 were prepared using similar strategies, only the preparation of AAV9-CMV_{enh}MLC800-3xFlag-ATF6α(1-373) is described here. The shuttle vector, pTRUF-CMV_{enh}MLC800, was constructed by modifying pTRUF12 (a gift from Dr. Roger Hajjar) by first removing the region encoding GFP that was down-stream of the IRES. New restriction sites were inserted into the multiple cloning site to include Nhe1, Pme1, Xho1, and Mlu1. The CMV promoter was replaced with a composite promoter comprised of an 800bp fragment of the MLC2v promoter downstream of a minimal region of the CMV enhancer (a gift from Dr. Oliver J. Muller). AAV9 vectors with wild-type capsids were generated by co-transfection of the helper plasmid, pDG-9. pTRUF-CMV_{enh}MLC800-3xFlag-ATF6α(1-373) was created by sub-cloning the human 3xFlag-ATF6 a (1-373) cDNA from pcDNA3.1-3xFlag-ATF6α(1-373). To prepare the recombinant AAV9, HEK293T cells were plated a density of $8x10^6$ per T-175 flask and maintained in DMEM/F12 containing 10%FBS, penicillin/streptomycin at 37°C and 5% CO_2. For each virus preparation, 48 flasks were used. Twenty-four hours after plating, cultures were transfected using Polyethylenimine "Max" (MW 40,000, Polysciences, cat# 24765) as follows: For each T-175 flask, 15µg of helper plasmid and 5µg of pTRUF plasmid were mixed with 1 ml of DMEM:F12 (no antibiotics) and 160 µl of polyethylenimine (0.517 mg/ml), vortexed for 30 seconds, and incubated for 15 min at room temperature. This was then mixed with 18 ml DMEM/F12 containing 2% FBS, penicillin/streptomycin then used to replace the media on the cultures. The cultures were then rocked intermittently for 15 minutes before incubation. Three days after transfection, the cells collected from six T-175 flasks were centrifuged at 500xg for 10 min, then resuspended in 10 ml of lysis buffer (150 mM NaCl, 50 mM Tris-HCL). The resuspended cells were then subjected to three rounds of freeze-thaw, followed by treatment with benzonase (1500 U of benzonase; Novagen) and 1 mM $MgCl_2$ at 37°C for 30 min. The cell debris was collected by centrifugation at 3,400 x g for 20 min. The supernatant obtained from six T-175 flasks containing the AAV9 was then purified on an iodixanol gradient comprised of the following four phases: 7.3 ml of 15%, 4.9 ml of 25%, 4 ml of 40%, and 4 ml of 60% iodixanol (Optiprep; Sigma-Aldrich) overlayed with 10 ml of cell supernatant. The gradients were centrifuged in a 70Ti rotor (Beckman Coulter) at 69,000 rpm for 1h using OptiSeal Polyallomer Tubes (Beckman Coulter). Virus was collected by inserting a needle 2 mm below the 40%-60% interface and collecting 4 or 5 fractions (~4ml) of this interface and most of the 40% layer. The fractions were analyzed for viral content and purity by examining 10 µl of each fraction on a 12% SDS-PAGE gel (BioRad), followed by staining with InstantBlue (Expedeon) to visualize the viral capsid proteins, VP1, VP2 and VP3. The virus was then collected from the fractions of several gradients and the buffer was exchanged with lactated Ringer's using an ultrafiltration device, Vivaspin 20, 100kDa MWCO (GE Healthcare). The final viral preparation was then fractionated on a 12% SDS-PAGE gel, stained with InstantBlue, and then compared with a similarly stained gel of a virus of a known titer. Alternatively, a qPCR was performed using a forward primer (AAGTCTCCACCCCATTGACGT) and reverse primer (AGGAGCCTGAGCTTTGATTCC), which spans the CMV_{enh}MLC800 composite promoter. A pTRUF vector containing the CMV/MLC800 promoter was used as a

standard to determine copy number. pTRUF-CMV$_{enh}$MLC-empty was used to generate an analogous control virus.

Cloning and mutagenesis

The promoter region of the rat catalase gene spanning nucleotides -1161 to +131 was amplified by PCR using ggaacgGGTACCTCACTGCCTTTATGGGCTTC as the forward primer, which introduced a Kpn1 site (lower case) just 5' of rat catalase -1161, and ggaacgCTCGAGGTGTAGGATTGCGGAGCTG as the reverse primer, which introduced an Xho1 site just 3' of rat catalase +131. Upper case nucleotides match those in the rat catalase gene. The amplified product was then cloned into pGL2p to generate rat-cat(-1161/+131)-Luc. Truncated versions of rat-cat luciferase were cloned into pGL2p using a similar strategy and the same reverse primer coupled with the following forward primers:

ggaacgGGTACCAAAGGAGCCATGAAGCTGAA (-689),
ggaacgGGTACCACAGTGGGCCAAGTGACAAG (-410), and
ggaacgGGTACCGTCCCCGAACTGTGACTCTC (-191)

to generate rat-cat(-689/+131)-Luc, rat-cat(-410/+131)-Luc and rat-cat(-191/+131)-Luc, respectively. The underlined regions of these primers correspond to rat catalase gene sequences. Informatics analyses identified putative ER stress response elements in the rat catalase gene at nucleotide positions -979 to -962 and -194 to -184 in the rat catalase gene, which we called ERSE-2 and ERSE-1, respectively. These elements in rat-cat(-1161/+131)-Luc were mutated by site-directed mutagenes in ways predicted to ablate ATF6 binding using cat-ERSE-2 mut sense primer,

CCCAAGGGATTGCAAACTTACAATTTTACCccgCTCTGTTACCcacTCTTTGTCAAATC
AAGAACAAGTTTTGGAGT

and cat-ERSE-2 mut antisense primer,

ACTCCAAAACTTGTTCTTGATTTGACAAAgagTGGGTAACAGAGcggGGTAAAATTGT
AAGTTTTGCAATCCCTTGGG

cat-ERSE-1 mut sense primer,

CGTTGCACAGAGGAcggttTaaCagAACTGTGACTCTCAG, and

cat-ERSE-1 mut antisense primer,

CTGAGAGTCACAGTTctGttAaccgTCCTCTGTGCAACG.

PCR-based mutagenesis was performed using the QuikChange XL Site-Directed Mutagenesis Kit (Agilent Technologies, Santa Clara, CA). Lower case letters represent mutated nucleotides; upper case letters represent nucleotides that are identical to those in the rat catalase gene.

Luciferase reporter assay

Suspended NRVMs were co-transfected by electroporation with one of the above reporter constructs along with pCH110 plasmids encoding SV40-beta-galactosidase

and pGL2B, as described previously.[5] NRVMs were plated overnight and then infected with different forms of AdV-ATF6, as described above. NRVMs were lysed after 48 h, and the activities of luciferase and beta-galactosidase were measured using an Optocompt II luminometer (MGM Instruments, Hamden, CT) as described previously[6].

Chromatin immunoprecipitation (ChIP)

ChIP assays were performed essentially as previously described[11]. Briefly, AdV-FLAG-ATF6 form 1-infected NRVM (2 x 10^6 cells) were treated with fixing buffer (50 mM HEPES-KOH, pH 7.5, 100 mM NaCl, 1 mM EDTA, 0.5 mM EGTA, and 1% formaldehyde) for 10 min, quenched with 125 mM glycine, and scraped into ice-cold PBS. Cells were centrifuged, resuspended in lysis buffer (50 mM HEPES, pH 7.9, 140 mM NaCl, 1 mM EDTA, 10% glycerol, 0.5% NP-40, 0.25% Triton X-100, and protease inhibitor cocktail), and incubated on ice for 10 min. After centrifugation at 1,800 x g for 10 min, the pellets were washed with buffer containing 10 mM Tris, pH 8.1, 200 mM NaCl, 1 mM EDTA, and 0.5 mM EGTA, resuspended in shearing buffer (0.1% SDS, 1 mM EDTA, and 10 mM Tris, pH 8.1), and then transferred to microTUBEs (Covaris, Woburn, MA). Chromatin was sheared by sonication for 15 min using an M220 focused-ultrasonicator (Covaris). Triton X-100 and NaCl were added to the final concentration of 1% Triton and 150 mM NaCl followed by centrifugation at 16,000 x g for 10 min. Immunoprecipitation was performed by incubated 140 µl of sheared chromatin with 5 µg of anti-FLAG antibody (cat# F1804, Sigma-Aldrich) and 260 µl of immunoprecipitation buffer (0.1% SDS, 1 mM EDTA, 10 mM Tris, pH 8.1, 1% Triton X-100, and 150 mM NaCl) at 4°C overnight. Protein A/G magnetic beads (5 µl, BcMag, Bioclone, San Diego, CA) were added to the mixtures and incubated at 4°C for 1.5 h. Magnetic beads were sequentially washed with low salt wash buffer (0.1% SDS, 1% Triton X-100, 2 mM EDTA, 20 mM HEPES-KOH, pH7.9, and 150 mM NaCl), high salt wash buffer with 500 mM NaCl, LiCl wash buffer (100 mM Tris-HCl, pH 7.5, 0.5 M LiCl, 1% NP-40, and 1% deoxycholate acid), and TE buffer (10 mM Tris-HCl, pH 8.0 and 0.1 mM EDTA). Immune complexes were eluted by incubating beads with proteinase K digestion buffer (20 mM HEPES, pH 7.9, 1 mM EDTA, 0.5% SDS, and 0.4 mg/ml proteinase K) at 50°C for 15 min. Formaldehyde crosslinking was reversed by incubating with 0.3 M NaCl and 0.3 mg/ml RNase A at 65°C overnight. Samples were further incubated with 550 µg/ml proteinase K at 50°C for 1h. DNA was purified using NucleoSpin Gel and PCR Clean-up Kit (Macherey-Nagel, Bethlehem, PA) and eluted by 30 µl of water. Two µl of DNA was used for qRT-PCR analysis with primers targeting rat Cat ERSE-1 (5'-CTACCCACCAATTAGTACCAAATAA-3' and 5'-AGAAGGGACAGGATTGGAAG-3'), rat Cat ERSE-2 (5'-CACATTCTAGGGACAGTGTAGATG-3' and 5'-ACCTTGATTATGGGCTGTGG-3') or the rat Pdia6 ERSE (5'-CACATGAGCGAAATCCACAGA-3' and 5'-ACTAGTCGAGCCATGCTGAT-3'). Pdia6 served as a positive control for a known ATF6 target gene in cardiac myocytes[11]. ChIP signals obtained from the qRT-PCR were normalized to the input DNA.

Supplemental References:

1. Doroudgar S, Volkers M, Thuerauf DJ, Khan M, Mohsin S, Respress JL, Wang W, Gude N, Muller OJ, Wehrens XH, Sussman MA, Glembotski CC. Hrd1 and ER-Associated Protein Degradation, ERAD, are Critical Elements of the Adaptive ER Stress Response in Cardiac Myocytes. *Circ Res.* 2015;117(6):536-546.

2. Thuerauf DJ, Morrison LE, Hoover H, Glembotski CC. Coordination of ATF6-mediated transcription and ATF6 degradation by a domain that is shared with the viral transcription factor, VP16. *J Biol Chem.* 2002;277(23):20734-20739.

3. Thuerauf DJ, Marcinko M, Gude N, Rubio M, Sussman MA, Glembotski CC. Activation of the unfolded protein response in infarcted mouse heart and hypoxic cultured cardiac myocytes. *Circ Res.* 2006;99(3):275-282.

4. O'Connell TD, Rodrigo MC, Simpson PC. Isolation and culture of adult mouse cardiac myocytes. *Methods Mol Biol.* 2007;357:271-296.

5. Pinz I, Zhu M, Mende U, Ingwall JS. An improved isolation procedure for adult mouse cardiomyocytes. *Cell Biochem Biophys.* 2011;61(1):93-101.

6. Doroudgar S, Thuerauf DJ, Marcinko MC, Belmont PJ, Glembotski CC. Ischemia activates the ATF6 branch of the endoplasmic reticulum stress response. *J Biol Chem.* 2009;284(43):29735-29745.

7. Sciarretta S, Zhai P, Shao D, Zablocki D, Nagarajan N, Terada LS, Volpe M, Sadoshima J. Activation of NADPH oxidase 4 in the endoplasmic reticulum promotes cardiomyocyte autophagy and survival during energy stress through the protein kinase RNA-activated-like endoplasmic reticulum kinase/eukaryotic initiation factor 2alpha/activating transcription factor 4 pathway. *Circ Res.* 2013;113(11):1253-1264.

8. Lynch JM, Maillet M, Vanhoutte D, Schloemer A, Sargent MA, Blair NS, Lynch KA, Okada T, Aronow BJ, Osinska H, Prywes R, Lorenz JN, Mori K, Lawler J, Robbins J, Molkentin JD. A thrombospondin-dependent pathway for a protective ER stress response. *Cell.* 2012;149(6):1257-1268.

9. Glembotski CC, Thuerauf DJ, Huang C, Vekich JA, Gottlieb RA, Doroudgar S. Mesencephalic astrocyte-derived neurotrophic factor protects the heart from ischemic damage and is selectively secreted upon sarco/endoplasmic reticulum calcium depletion. *J Biol Chem.* 2012;287(31):25893-25904.

10. Jin JK, Whittaker R, Glassy MS, Barlow SB, Gottlieb RA, Glembotski CC. Localization of phosphorylated alphaB-crystallin to heart mitochondria during ischemia-reperfusion. *Am J Physiol Heart Circ Physiol.* 2008;294(1):H337-344.

11. Vekich JA, Belmont PJ, Thuerauf DJ, Glembotski CC. Protein disulfide isomerase-associated 6 is an ATF6-inducible ER stress response protein that protects cardiac myocytes from ischemia/reperfusion-mediated cell death. *J Mol Cell Cardiol.* 2012;53(2):259-267.

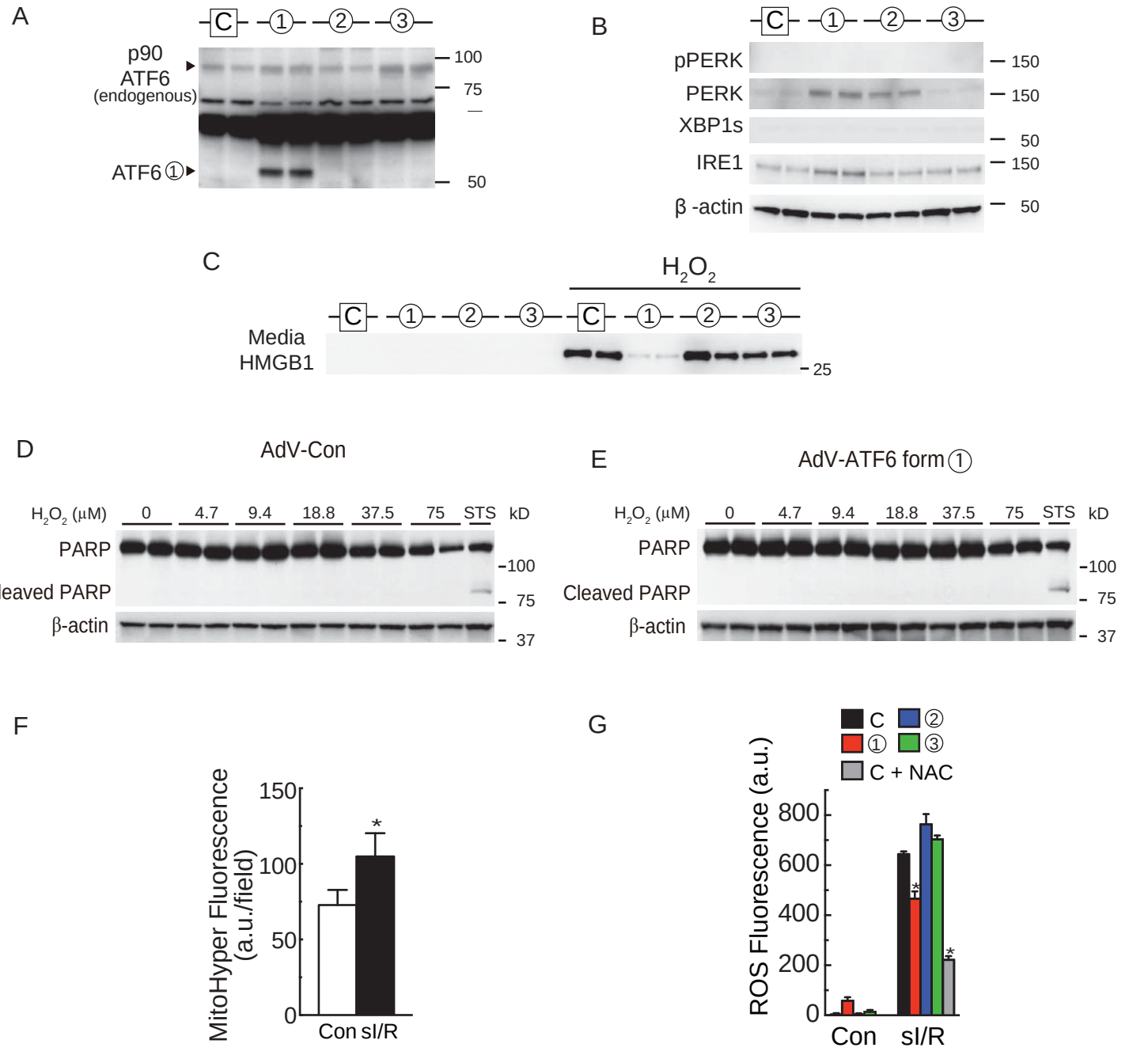

Online Figure I- Effect of AdV-ATF6 on ER Stress Signaling, HMGB1, H_2O_2 on PARP cleavage, and ROS in cultured cardiac myocytes: A, B, C, NRVM were infected with AdV encoding the forms of ATF6 shown then immunoblotted for ATF6 (A), phospho-PERK (pPERK), PERK, spliced XBP1 (XBP1s), IRE-1, and β-actin (B), or treated with H_2O_2 then immunoblotted for HMGB1 (C). **D, E,** NRVM were infected with AdV-Con, or AdV-ATF6 form 1, then treated for 8h with various concentrations of H_2O_2, as shown. As a positive control, NRVM were treated with staurosporine (STS; 1 μM) for 24h, which is known to induce apoptosis and not necrosis. Cultures were then extracted and subjected to immunoblotting for PARP using an antibody that detects intact and cleaved PARP. Blots were also probed for β-actin as a loading control. **F,** NRVM were infected with AdV-mito-HyPer, then subjected to either Control (Con) conditions, or sI/R after which fluorescence was measured. * p<0.05 different from Con. **G,** NRVM were infected with AdV-Con, or AdV encoding the forms of ATF6 shown, then subjected to either Con or sI/R and ROS were measured using Amplex Red. * p<0.05 different from all other values, by ANOVA.

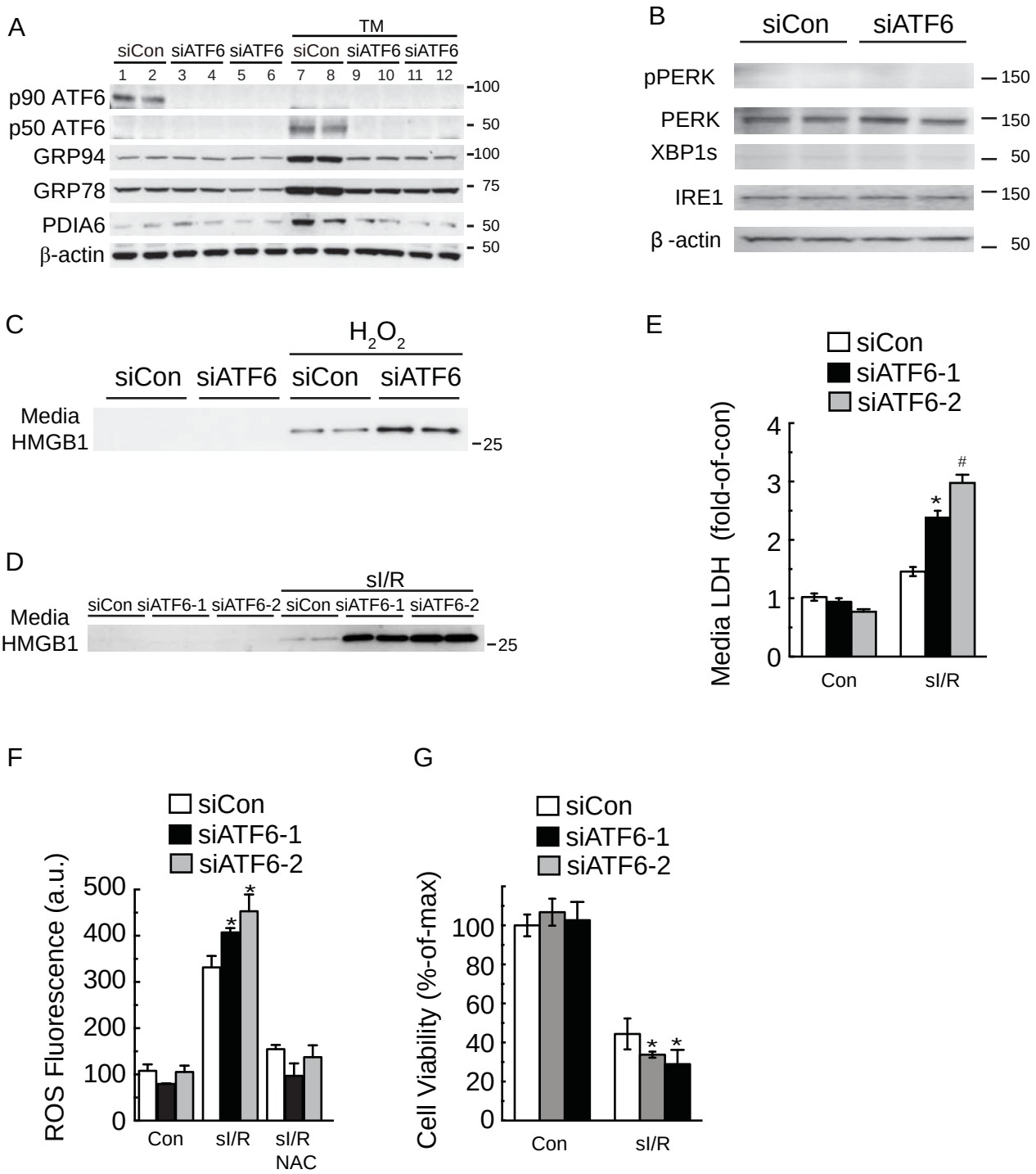

Online Figure II- Effect of ATF6 siRNA in NRVM: NRVM were transfected with siCon or two different ATF6-targeted siRNAs, siATF6-1 or siATF6-2 separately, where indicated, then either untreated, or treated with TM, sI/R or H_2O_2, as shown, then immunoblotted for the proteins shown, media measured for HMGB1 or LDH levels, ROS measured using an Amplex Red assay, or cell viability was measured using calcein AM blue staining. In E-G, * $p<0.05$ different from all other values in that treatment group by ANOVA.

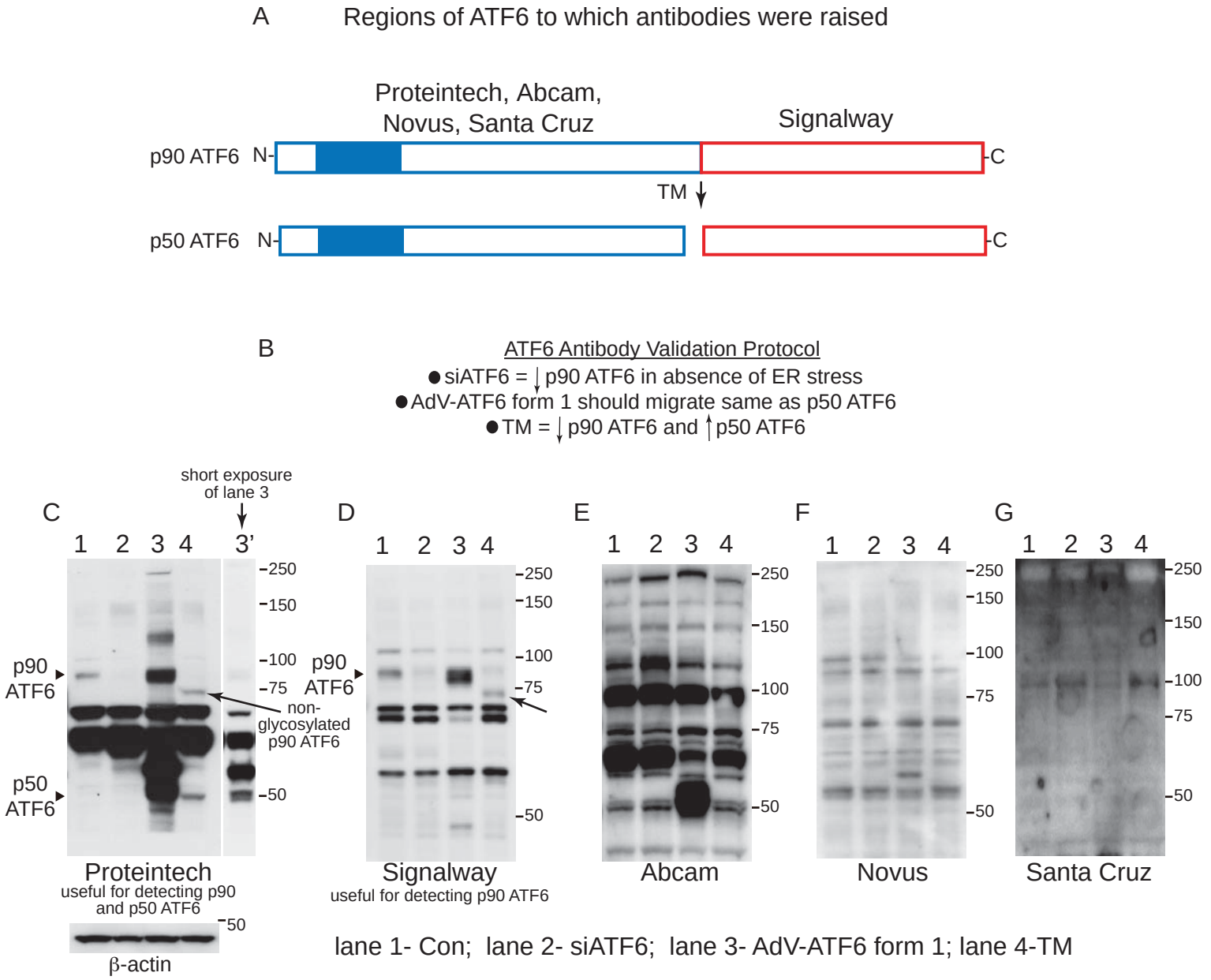

Online Figure III- Validation of ATF6 antibodies used for immunoblotting: A, Locations on ATF6 to which the antibodies used in this study were raised. **B,** ATF6 Antibody Validation Protocol. **C-G,** NRVM were either not transfected (Con; **lane 1**), or transfected with siRNA to rat ATF6 (siATF6; **lane 2**), infected with AdV-ATF6 form 1 (**lane 3**), or treated for 16h with TM (10 μg/ml; **lane 4**). Extracts were then analyzed for ATF6 by immunoblotting using the antibodies shown. The identities of p90 ATF6 and p50 ATF6 were based on the blot results and the ATF6 Antibody Validation Protocol. Note that overexpression of ATF6 form 1 serves as a control (C, lane 3), and a shorter exposure of this lane is shown as 3'. The arrow in C and D indicates the unglycosylated form of p90 ATF6 that appears when cells are treated with TM, an inhibitor of ER protein glycosylation. The identities of bands other than those marked as p90 or p50 ATF6, or unglycosylated p90 ATF6 are not known. The Abcam antibody detected p90 and p50 ATF6 but also crossreacted with other proteins at these same locations, so was not used in this study. The Novus and Stanta Cruz antibodies did not specifically detect p90 or p50 ATF6, so they were not used in this study.

Online Figure III

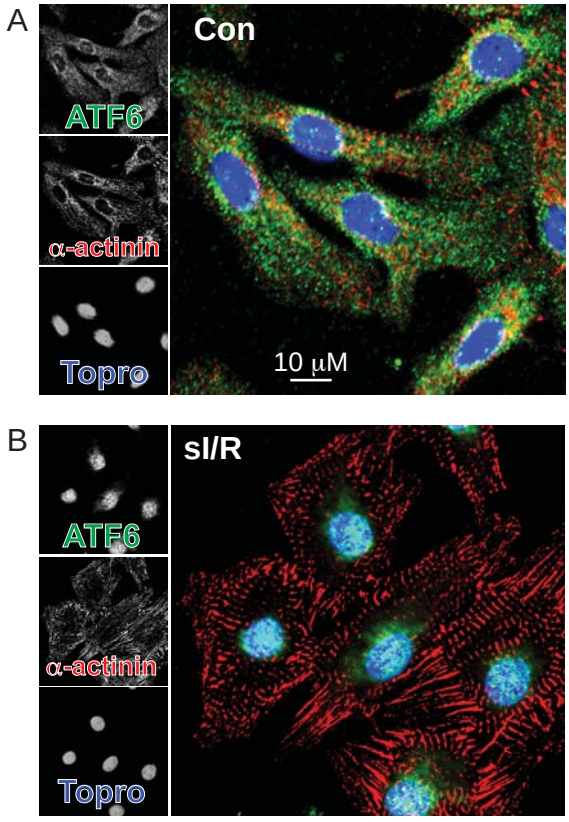

Online Figure IV- Effect of sI/R on ATF6 expression and localization in cardiac myocytes: NRVM were either untreated (Con; A), or treated for 4h with simulated ischemia followed by 24h of simulated reperfusion (sI/R; B), then fixed and stained for ATF6 (ATF6; green), α-actinin (red), or TOPRO (blue).

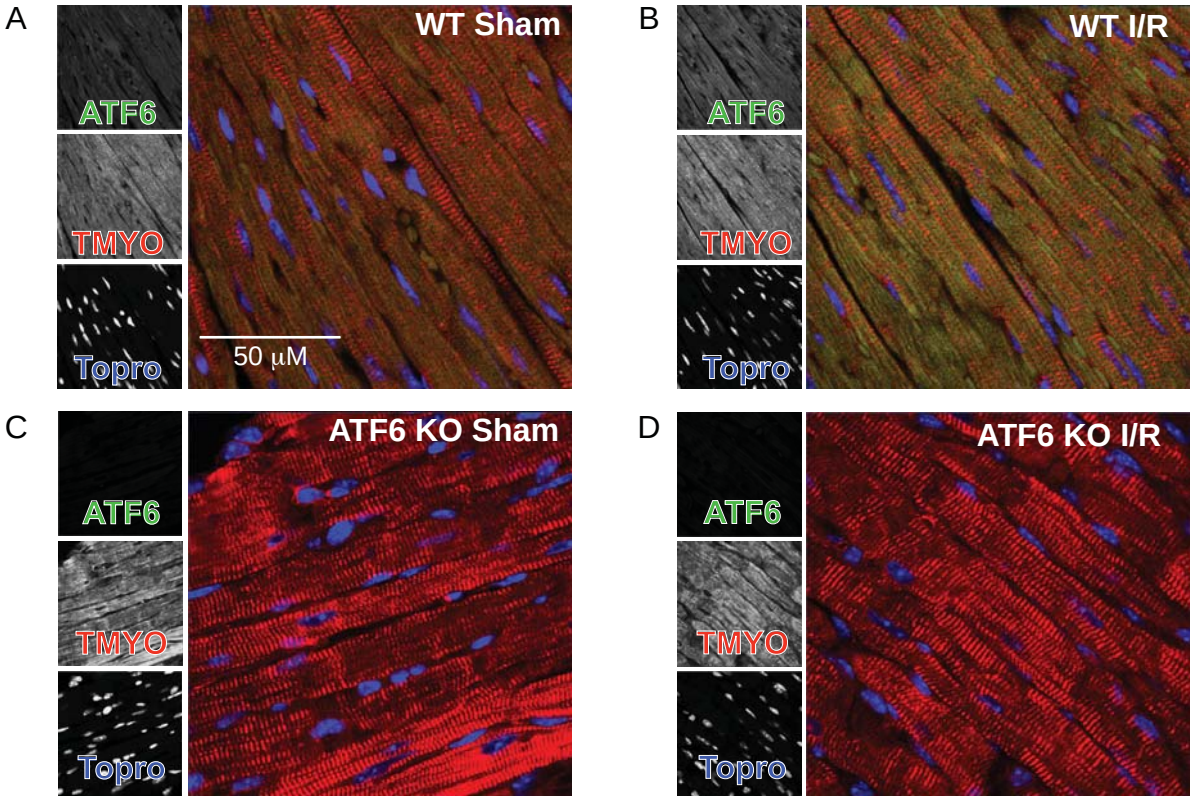

Online Figure V- Effect of I/R on ATF6 expression in WT and ATF6 KO mouse hearts as determined by immunocytofluorescence: A, B, WT or **C, D,** ATF6 KO mice were subjected to I/R *in vivo*, after which hearts were obtained and sections were stained for ATF6 (green), tropomyosin (red), or TOPRO (blue).

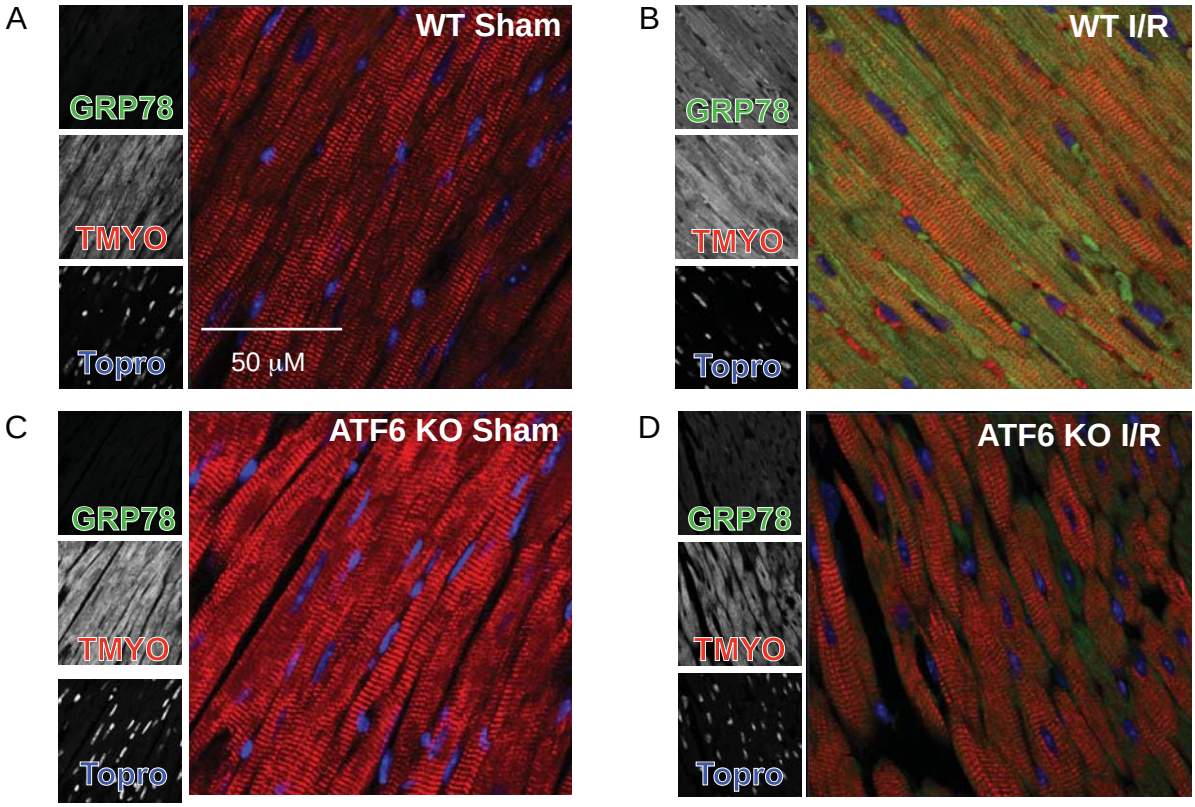

Online Figure VI- Effect of I/R on GRP78 expression in WT and ATF6 KO mouse hearts as determined by immunocytofluorescence: A, B, WT or **C, D,** ATF6 KO mice were subjected to I/R *in vivo*, after which hearts were obtained and sections were stained for GRP78 (green), tropomyosin (red), or TOPRO (blue).

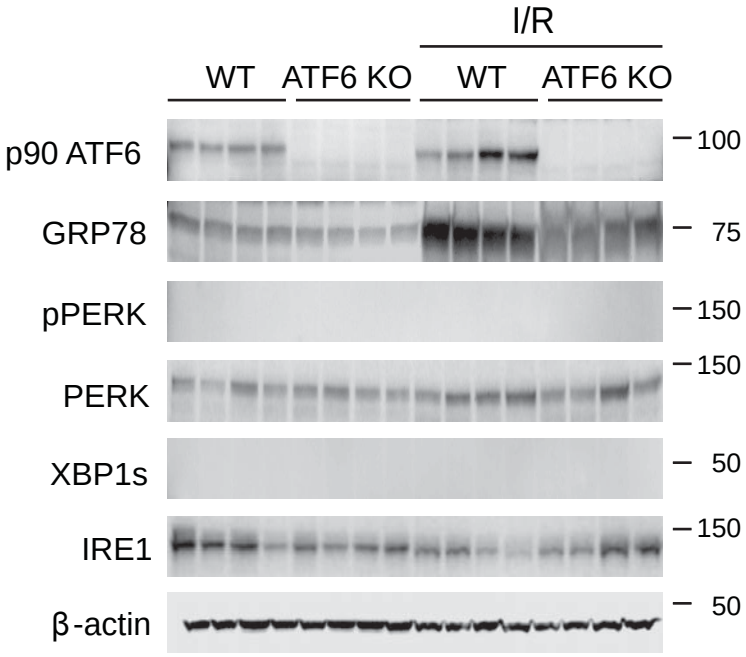

Online Figure VII- Effect of I/R on markers of ER stress in WT and ATF6 KO mouse hearts as determined by immunoblotting: WT or ATF6KO mice were subjected to I/R *in vivo*, after which hearts were obtained and extracts were immunoblotted for p90 ATF6, GRP78, phospho-PERK (pPERK), total PERK (PERK), spliced XBP1 (XBP1s), IRE-1 and β-actin.

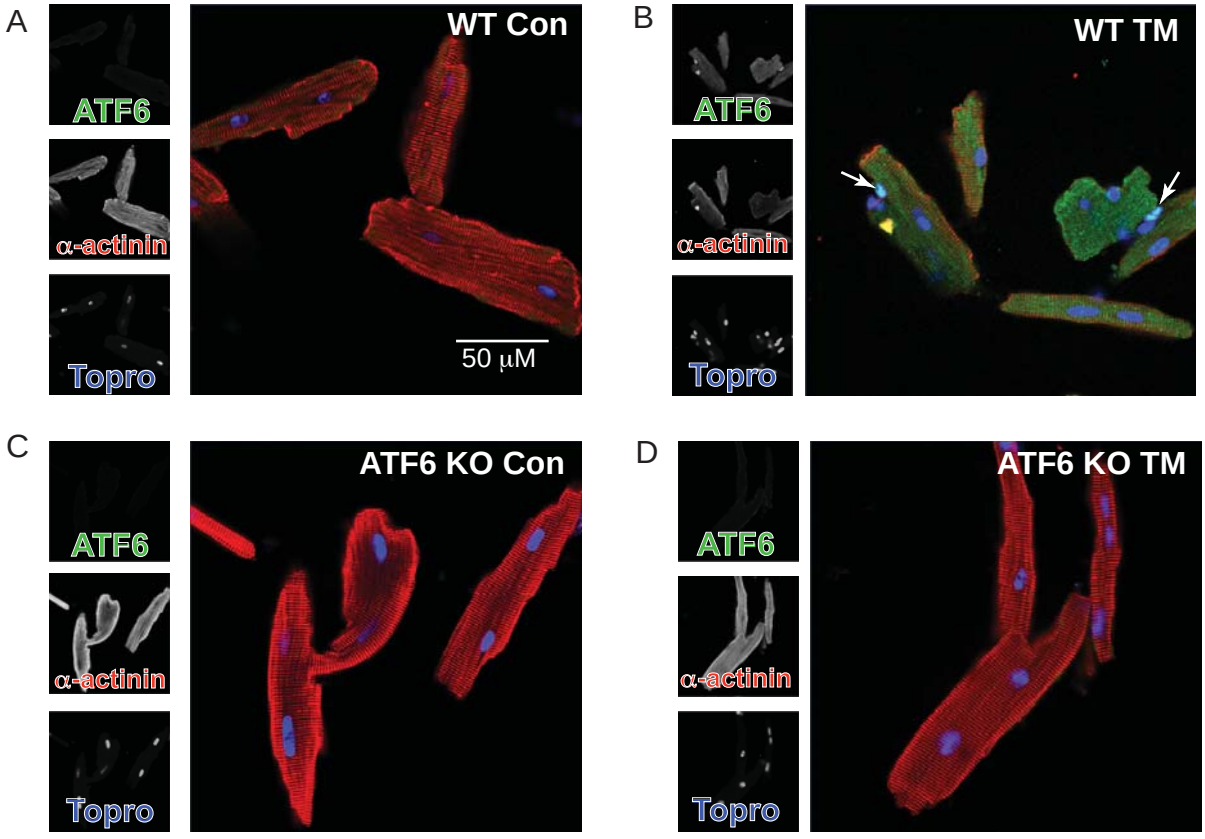

Online Figure VIII- Effect of TM on ATF6 expression in cardiac myocytes from WT and ATF6 KO mouse hearts: A, B, Myocytes were isolated from WT or **C, D,** ATF6 KO mouse hearts then treated without (A, C) or with TM (10 μg/ml; 24h; B, D), then fixed and stained for ATF6 (ATF6; green), α-actinin (red), or TOPRO (blue). Arrows in B point to ATF6-positive nuclei.

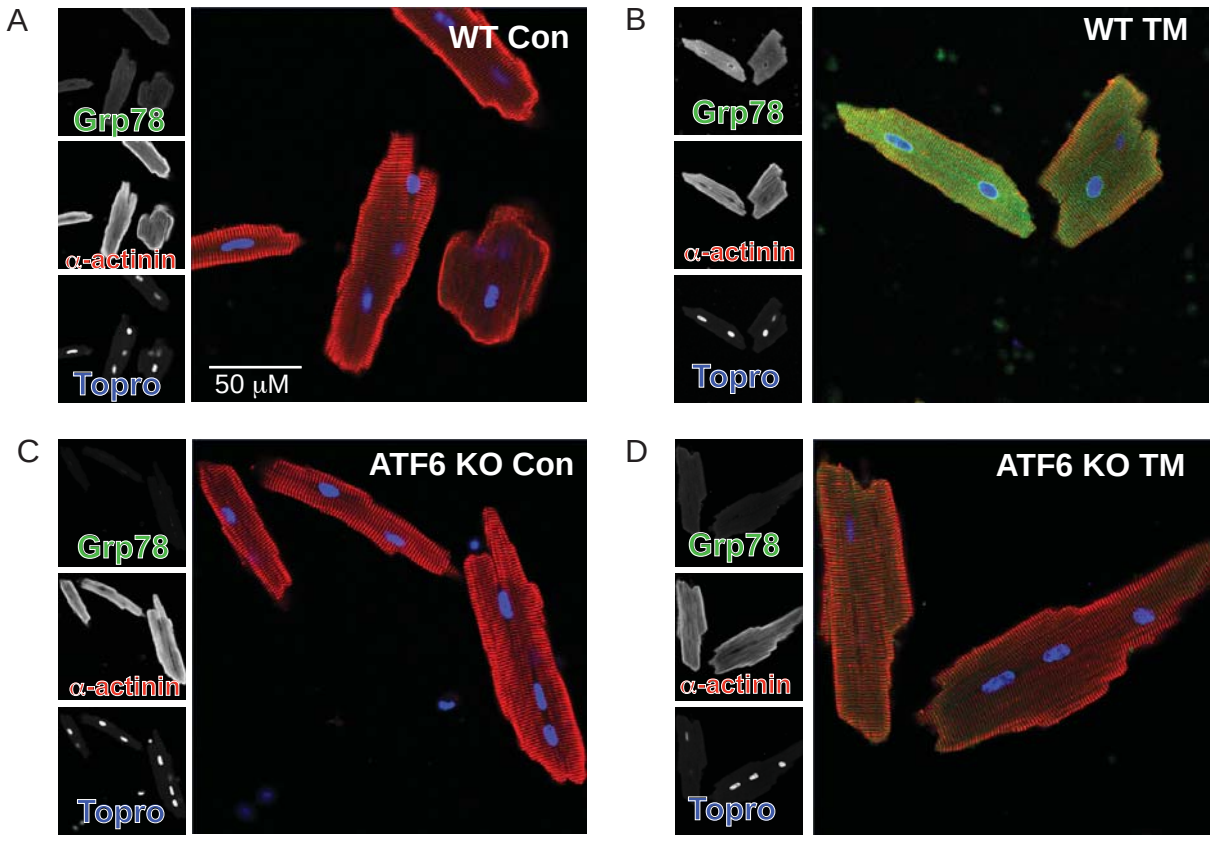

Online Figure IX- Effect of TM on GRP78 expression in cardiac myocytes from WT and ATF6 KO mouse hearts: A, B, Myocytes were isolated from WT or **C, D,** ATF6 KO mouse hearts then treated without (A, C) or with TM (10 μg/ml; 24h; B, D), then fixed and stained for GRP78 (green), α-actinin (red), or TOPRO (blue).

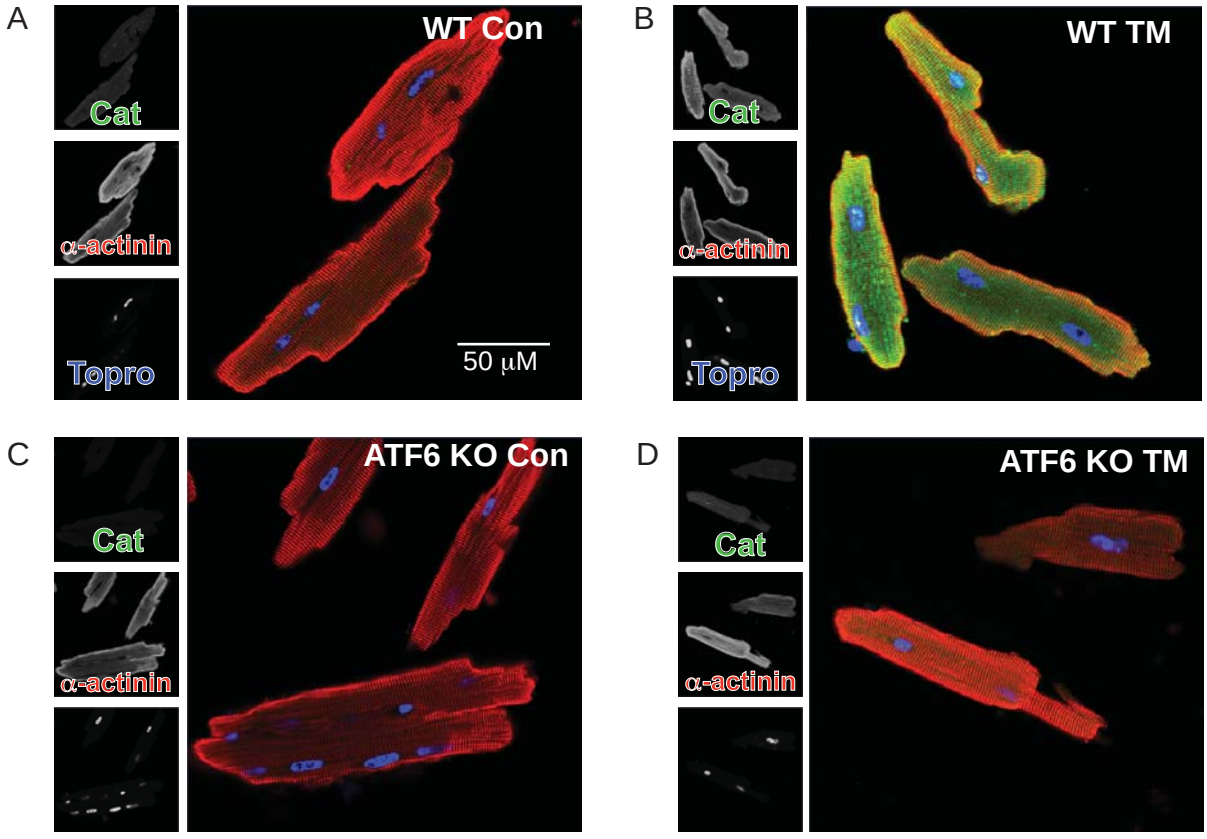

Online Figure X- Effect of TM on Catalase Expression in Cardiac Myocytes from WT and ATF6 KO Mouse Hearts: A, B, Myocytes were isolated from WT or **C, D,** ATF6 KO mouse hearts then treated without (A, C) or with TM (10 μg/ml; 24h; B, D), then fixed and stained for catalase (Cat; green), α-actinin (red), or TOPRO (blue).

Online Figure X

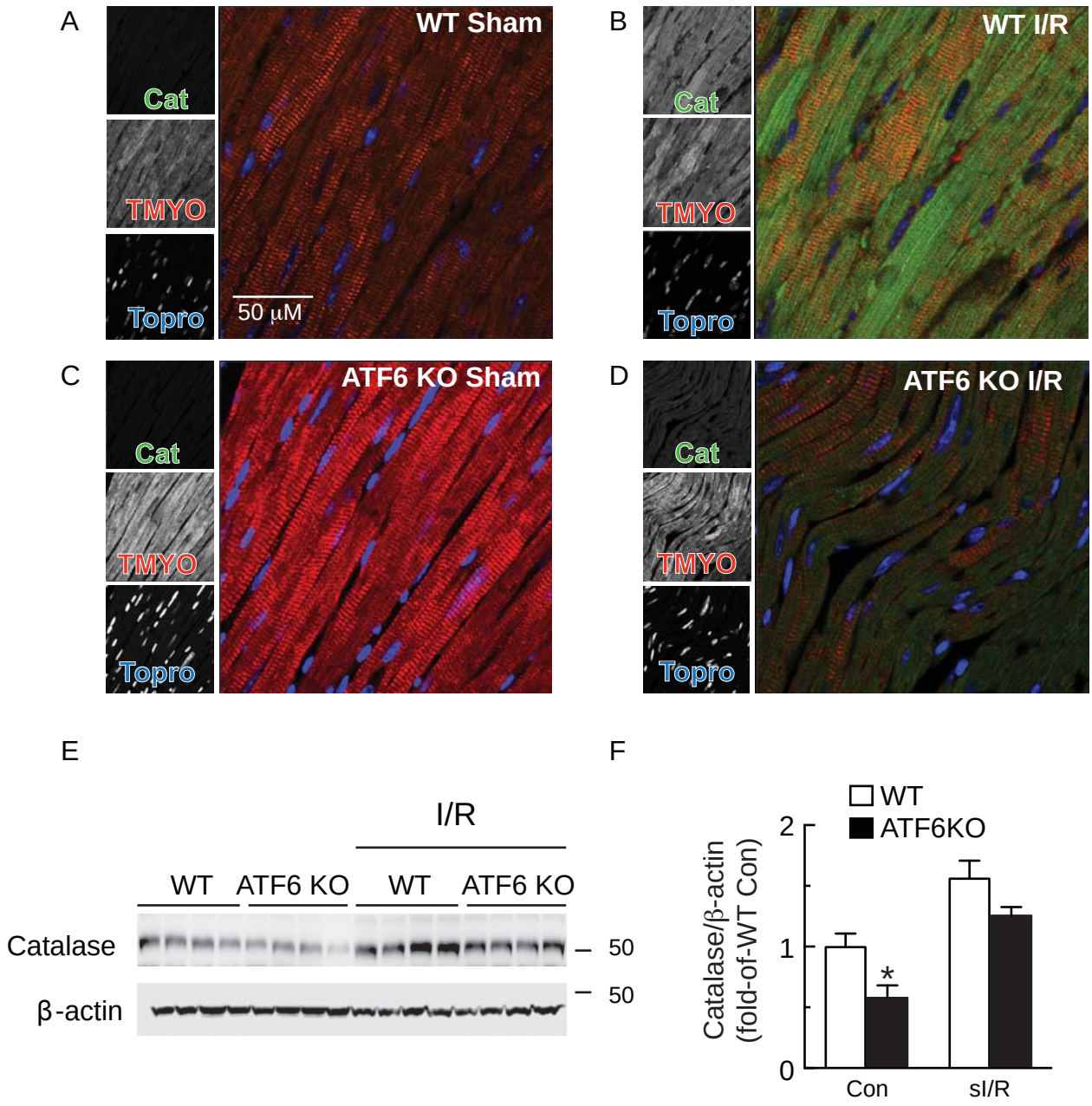

Online Figure XI- Effect of I/R on Catalase expression in WT and ATF6 KO mouse hearts as determined by immunocytofluorescence and immunoblotting: A, B, WT or **C, D,** ATF6 KO mice were subjected to I/R in vivo, after which hearts were obtained and sections were stained for Catalase (green), tropomyosin (red), or TOPRO (blue). **E,** Hearts from WT or ATF6 KO subjected to I/R in vivo were extracted and analyzed for catalase and β-actin by immunoblotting (n = 4 mice per treatment). **F,** The immunoblots shown in E were quantified by densitometry. * $p<0.05$ different from WT Con by t-test.

Online Table I: Echocardiograph results of 10 week-old WT and ATF6 KO mice

	WT 10 week old (n = 8)	ATF6 KO 10 week old (n = 8)
FS (%)	29.89±1.75	30.65±1.03
EF (%)	56.80±2.39	58.81±1.95
LVEDV (μl)	65.70±4.67	62.50±4.47
LVESV (μl)	28.56±3.47	25.88±2.62
LVIDD (mm)	3.87±0.12	3.85±0.11
LVIDS (mm)	2.78±0.12	2.70±0.09
PWTD (mm)	0.71±0.05	0.66±0.02
PWTS (mm)	1.03±0.07	1.04±0.03
AWTD (mm)	0.82±0.10	0.88±0.04
AWTS (mm)	1.19±0.09	1.24±0.06
LV mass (mg)	106.90±14.48	111.90±6.02
HR (bpm)	471.80±6.05	477.9±5.88
SV (μl)	37.11±1.75	35.56±2.38
CO (ml/min)	17.49±0.71	17.54±1.17

FS = fractional shortening
EF = ejection fraction
LVEDV = left ventricular end diastolic volume
LVESV = left ventricular end systolic volume
LVIDD = left ventricular inner diameter in diastole
LVIDS = left ventricular inner diameter in systole
PWTD = left ventricular posterior wall thickness in diastole
PWTS = left ventricular posterior wall thickness in systole
AWTD = left ventricular anterior wall thickness in diastole
AWTS = left ventricular anterior wall thickness in systole
LV mass = left ventricular mass
HR = heart rate in beats per minute
CO = cardiac output
SV = stroke volume

None of the parameters were significantly different between WT and ATF6 KO mice as determined by t-test

Online Table II

Oxidative Stress Response Genes Increased or Decreased by ATF6 in Cardiac Myocytes

No	Gene	Accession	Protein name	Location	Notes	Se[1]	Up/Dn
1	Als	P0C5Y8	Rho guanine nucleotide exchange factor	cytoplasm			Up
2	Cat	P04762	Catalase	peroxisome	metabolizes H_2O_2		Up
3	Dnm2	P39052	Dynamin-2	cytoplasm			Up
4	Epx	D3Z5Y4	Eosinophil peroxidase	extracellular	secreted in exosomes		Up
5	Gpx3	P23764	Glutathione peroxidase 3	ER; secreted	classically secreted metabolizes H_2O_2	X	Up
6	Gpx4	P23764	Glutathione peroxidase 4	mitochondria	mitochondria/cytosol metabolizes peroxylipids	X	Up
7	Nqo1	P05982	NAD(P)H quinone dehydrogenase	cytoplasm			Up
8	Prdx5	Q9R063	Peroxiredoxin-5	mitochondria peroxisomes	has mito and peroxisome targeting sequences	X	Up
9	Vimp	A0G2K953	VCP-interacting membrane Se-protein	cytoplasm; ER	has an ER transmembrane domain	X	Up
10	Slc38a1	Q9JM15	Solute carrier family 38, member 1	cell mem			Up
11	Txnrd1	O89049	Thioredoxin reducatase 1	cytoplasm		X	Up
12	CCl5	P50231	C-C motif chemokine 5	secreted	classically secreted		Dn
13	Cyba	Q62737	Cytochrome b-245 light chain	cell mem	NADHP oxidase component generates ROS		Dn
14	Cygb	Q921A4	Cytoglobin	cytoplasm	metabolizes H_2O_2		Dn
15	Mb	Q9QZ78	Myoglobin	extracellular	secreted in exosomes		Dn
16	Ncf1	F1M707	Neutrophil cytosolic factor 1	cell mem	required for superoxide production		Dn
17	Serpinb1b	F8WGA3	Protein serpinb1b	secreted	serine protease inhibitor		Dn
18	Ucp2	P56500	Uncoupling protein 2	mito			Dn

[1]Se = Selenoprotein